ASSESSMENT OF A DEEP, LED-ENHANCED HIGH-RATE ALGAL POND FOR THE TREATMENT OF DIGESTATE

Torres-Franco, A.F.[1], Figueredo, C. C.[2], Barros L.[1], Gücker B.[3], Boëchat, I.G.[3], Muñoz R.[4,5], Mota, C.R.[1] *

[1]*Department of Sanitary and Environmental Engineering, Federal University of Minas Gerais-Belo Horizonte 31270-010, Brazil;*

[2]*Institute of Biological Sciences, Federal University of Minas Gerais Belo Horizonte 31270-010, Brazil;*

[3]*Department of Geosciences, Federal University of São João del-Rei, Praça Dom Helvécio 74, São João del-Rei, MG 36301-160, Brazil;*

[4]*Department of Chemical Engineering and Environmental Technology, School of Industrial Engineering, Valladolid University, Dr. Mergelina s/n., Valladolid 47011, Spain;*

[5]*Institute of Sustainable Processes, Valladolid University, Dr. Mergelina s/n., Valladolid 47011, Spain.*

*-*Corresponding author: cesar@desa.ufmg.br*

Abstract. High Rate Algal Ponds (HRAP) are a sustainable alternative for wastewater treatment. However, HRAPs must be shallow (h=0.2-0.3 m) for adequate sunlight penetration and require relatively long hydraulic retention times (HRT, >5 d) for effective pollutant removal, which results in high area footprints. In this context, a deep HRAP (h=1.2 m) was equipped with red light-emitting diodes (LED, 660 nm) to provide photosynthetic active radiation in the aphotic zone. A conventional HRAP ($HRAP_1$) and the LED-enhanced HRAP ($HRAP_2$) were operated with identical working volumes (1.25 m^3) and HRT (10 d), treating digestate dilutions of 5% (Stages S-0, S-I), 25% (S-II, S-III) and 50% (v/v) (S-IV to S-VI). The $HRAP_2$ used only 25% of the area needed by the $HRAP_1$ but LEDs used 1.4 (S-0 to S-II), 2.3 (S-III, S-IV) and 3.4 (S-V) times the energy consumed in $HRAP_1$. $HRAP_2$ presented similar performance to $HRAP_1$ during the treatment of 5% and 25%-digestate, achieving removals above 75% for TSS, COD, TAN, and TKN. However, $HRAP_1$ showed better treatment performance at 50%-digestate, likely due to more intense light radiation induced by its shallow depth, resulting in higher microalgal activity. Biomass productivity decreased with increasing digestate concentration, showing averages in $HRAP_1$ and $HRAP_2$ of 9 and 3 $gVSS \cdot m^{-2}d^{-1}$, respectively, during feeding with 5%-digestate. With 25%, average productivities ranged from 2 to 5 and 2 to 6 $gVSS \cdot m^{-2}d^{-1}$, and from 0 to 6 and 0 to 4 $gVSS \cdot m^{-2}d^{-1}$ with 50%-digestate, respectively. Both systems showed reasonable nitrogen and phosphorus recoveries in the biomass (TN: 8-17% and 6-34%; TP: 10-45% and 5-48% for $HRAP_1$ and $HRAP_2$, respectively). Nitrogen volatilization, likely as NH_3, N_2O, and N_2, was caused by stripping and nitrification-denitrification in both systems. Our data suggest that using LED-lighting to complement sunlight in deeper HRAPs is a promising alternative for enhancing microalgae-based reactors for digestate treatment.

Keywords: Microalgae; LED lighting; wastewater treatment, nutrient removal and recovery; digestate

1 Introduction

The treatment of high-strength digestates coupled with microalgae cultivation can be a feasible alternative to achieve high pollutant removal efficiencies coupled with resource recovery from wastewaters (Marin *et al*., 2018; Torres-Franco *et al.* 2020). Microalgae-based technologies, typically implemented in High-Rate Algal Ponds (HRAPs), can be an efficient, cost-effective wastewater treatment alternative due to their low operational costs and highly value-added biomass production (Uggetti *et al*., 2018). Nevertheless, their requirement for shallow depths and relatively long hydraulic retention times (Kim *et al*., 2018) results in large areal footprints, which is a major disadvantage of HRAPs when compared to other treatment technologies in an urban context where the price of land may be prohibitive (Garfí *et al*., 2017).

Reducing the area footprint of HRAPs may increase their applicability in the treatment of a wide variety of effluents. Slightly deeper ponds (0.3-0.5 m) or shorter HRTs have been tested with promising results (Sutherland *et al*., 2014; Hom-Diaz *et al*., 2017; Anbalagan *et al*., 2018; Kim *et al*., 2018), but ponds deeper than 0.5 m could be efficient only if coupled to artificial lighting, complementing sunlight availability for microalgae in the aphotic zone. Light-emitting diodes (LEDs) have been applied in microalgae-based wastewater treatment with promising results and a low energy consumption (Yan *et al*., 2016). Particularly, red LEDs are more attractive than other monochromatic LEDs since they exhibit higher photosynthetic active radiation (PAR) efficiency (Blanken *et al*., 2013) and an emission spectrum that matches the critical absorption peaks of chlorophyll a and b, which renders red LEDs the most adequate for photosynthesis (Jeon *et al*., 2005). In addition, renewable energies have the potential to power LED lighting, thus reducing their operational cost and environmental impact (Jankowska *et al*., 2019; Danyali *et al*., 2020).

Previous experiments have suggested the potential of low-intensity red LEDs to support chlorophytes' growth during the treatment of digestates without external CO_2 addition (Torres-Franco *et al*., 2018; Webb *et al*., 2019). However, there is little information on the performance of systems that combine sunlight and LED lights for the treatment of real digestate under outdoor conditions. In this study, a conventional HRAP ($HRAP_1$) and a LED-enhanced deep high-rate algal pond ($HRAP_2$) were compared in terms of their performance in the treatment of high-strength digestate (*i.e*., diluted food waste digestate). Both HRAPs were designed with the same working volume of 1.25 m^3 and operated with an HRT of 10 days. Mass balances were used to assess carbon and nutrients transformations and removals. Microalgae concentrations and energy consumption were also monitored to evaluate the performance of the LED-enhanced HRAP.

2 Material and methods

2.1 Experimental set-up

The conventional ($HRAP_1$) and the modified ($HRAP_2$) pilot ponds (Fig. 1) treated the digestate produced in a biomethanization system fed with 500 kg of food waste per week at Pampulha Campus of the Federal University of Minas Gerais (UFMG) in Belo Horizonte, Brazil (19°52'11.04'' S, 43°57'42.92" W). Both HRAPs were constructed with the same volume (V= 1.25 m^3), channel width:length ratio (1:6) and stainless-steel paddlewheels providing a mean velocity of ~0.2 $m \cdot s^{-1}$. Each pond's effluent was conducted to dedicated 750 L lamellar settlers, from which a pump recycled 75 $L \cdot d^{-1}$ (50% of the influent flow rate) of settled biomass to each HRAP. $HRAP_1$ was constructed with a depth (h) of 0.30 m, an area (A) of 4.2 m^2, a channel width (w) of 0.6 m, and sunlight as the only PAR source. $HRAP_2$ was designed with only 25% of the area of $HRAP_1$, a h of 1.20 m and a w of 0.3 m. To provide light to $HRAP_2$'s aphotic zone, a lateral panel of red LED lights was installed (SD 5050, 6 strips×15 W/m, 660 nm, 450 W, 40×90

cm), which constantly provided a PAR of 10-50 $\mu mol \cdot m^{-2} \cdot s^{-1}$ and was selected based on previous bench-scale experiments (Torres-Franco *et al*., 2018). After 180 days of operation, two additional panels of red LED lights with a wattage of 450 W and 600 W (SD 5050, 660 nm, 6 strips×15 W/m and 8 strips×15 W/m, respectively) were installed inside a glass box immersed in the opposite loop of $HRAP_2$. These additional panels were implemented to supply extra LED light irradiation due to the increase in digestate concentrations and the higher biomass concentrations in $HRAP_2$. The total wattage supplied by the three panels was 1500 W. Electricity consumption in the two HRAPs was measured with a WEG E34A (Brazil) electricity meter.

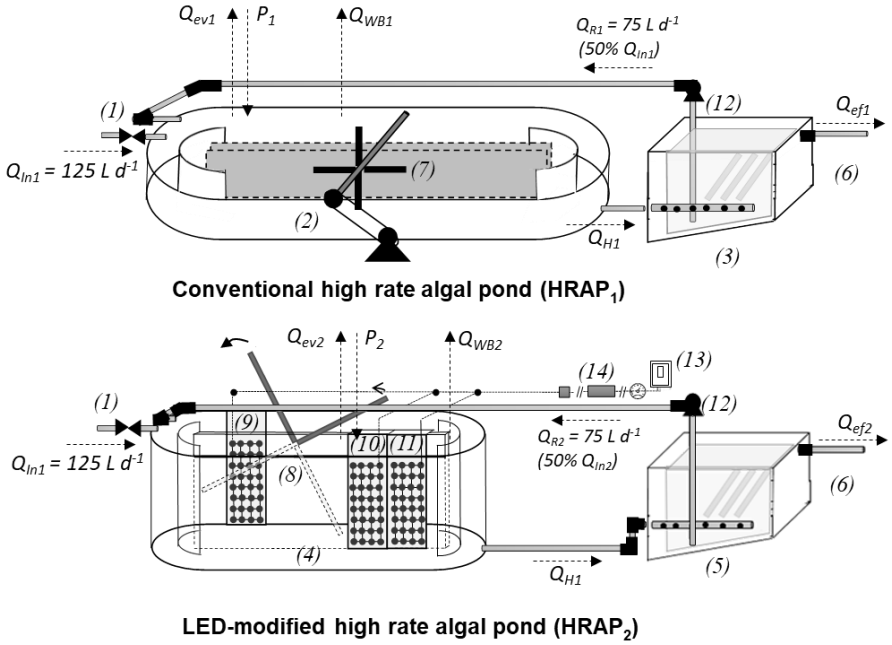

Figure 1 – Schematic representation of $HRAP_1$ and $HRAP_2$ with (1) digestate inlets; (2) conventional HRAP and dedicated (3) lamellar settler; (4) LED-modified HRAP and dedicated (5) lamellar settler; (6) effluent pipelines; (7) paddlewheel of the $HRAP_1$ (6- 0.55×0.1 m blades); (8) paddlewheel of the $HRAP_2$ (4- 0.2×0.45 m blades), (9) and (10) LED panels (450 W, SD 5050, 660 nm); (11) LED panel (600 W, SD 5050, 660 nm); (12) recirculation pumps; (13) WEG E34A meter; (14) 30A transformers × 3.

2.2 Digestate and microalgae inoculum

The digestate used in this study was a food waste digestate generated in the biomethanization reactor of the UFMG. The system comprised a 30 m^3 completely stirred anaerobic reactor

(CSAR) followed by a UASB reactor, whose effluent was treated in the HRAPs. Before being fed to the HRAPs, the digestate was settled for 24 h and then the supernatant was collected and used to prepare the daily feedings by mixing with tap water in order to achieve dilutions of 5%, 25%, and 50% (v/v). Digestate dilutions were prepared in two plastic tanks (V=500 L each) provided with an inner geotextile membrane (NF G 38016, pore diameter of 160 μm) to filter the diluted digestate by gravity prior to feeding the HRAPs. The diluted digestate in both tanks was homogenized to get the same influent concentrations to both HRAPs. Homogenization was controlled using a settleable solids test in Imhoff cones, ensuring the same solids volumes and visual appearances of both influents.

At the beginning of the experiment, HRAPs were inoculated with a mixture of 400 L of biomass from a maturation pond treating domestic wastewater located in Belo Horizonte (Brazil) and 400 L of water from an urban reservoir in the same city. The maturation pond was dominated by *Euglena* sp., *Scenedesmus* sp. and *Chlorella vulgaris*, whereas the urban reservoir water had a higher species diversity, including different species of *Scenedesmus* and *Euglena*, *Chlorella vulgaris*, *Dinobryon* sp., *Monactinus simplex*, *Botryococcus braunii*, *Pandorina* sp., *Planktolyngbya limnetica*, *Aulacoseira granulata*, *Peridinium* sp., *Desmodesmus* sp., *Trachelomonas volvocina,* and *Microcystis aeruginosa*. Both inocula were mixed and homogenized in $HRAP_2$ with tap water to complete 1.2 m^3. Subsequently, 600 L of this mixture was pumped to $HRAP_1$ and daily feedings with 5%-digestate started. Subsequently, the valves connecting the ponds with the settlers (initially filled with tap water) were opened, and operation was started.

2.3 Experimental design

The performance of both HRAPs was assessed for 586 d in operational stages based on step increases in influent digestate load (v/v) (Table 1): *i.e.*, 5% (Stage I, S-I), 25% (Stages II and III, S-II and S-III), and 50% (Stages IV to VI, S-IV to S-VI). The ponds were operated at a nominal hydraulic retention time (HRT) of 10 d. The start-up period (Stage 0, S-0) of the HRAPs was included in the assessment and defined as the period between the inoculation and the achievement of biomass concentrations in the recirculation line of ~2-fold the VSS of the HRAPs. Table 1 also shows the main characteristics of each stage, with a LED light supply in $HRAP_2$ of 450W during S-0, S-I and S-II; 900W during S-III and S-IV, and of 1500W during S-V. The LED panels were operated with a photoperiod of 24 h, but lights were turned off for 5 minutes each 4 hours to allow cooling of the panels. S-VI corresponded to a control stage without LED lighting in $HRAP_2$. Sunlight was the only PAR source in $HRAP_1$ throughout all stages. Digestate dilutions were prepared on a daily basis and gravity-fed to the HRPAs, continuously producing clarified effluent in the settlers. The effluent outlet hydraulically controlled the maximum depth of the HRPAs, whereas rainfall and evaporation resulted in gradual increases or draw down of pond volumes. Digestate availability was determined by the operation of the methanization bioreactor, which itself was determined by food waste availability. Therefore, the days with no digestate feeding were considered to calculate the actual flow rate (Q_a) and actual hydraulic retention time (HRT_a) of each stage (i) (Eq. 1 and Eq. 2):

$$Q_{a,\,i} = \frac{\text{Total Volume fed during each stage}}{\text{Number of days of each stage}} \quad \text{(Eq. 1)}$$

$$HRT_{a,i} = \frac{1.25\ \text{m}^3}{\text{Q}_\text{a}} \quad \text{(Eq. 2)}$$

Table 1. Main operational and environmental parameters in the different operational stages (Mean±S.D)

Stage	S-0	S-I	S-II	S-III	S-IV	S-V	S-VI
Digestate dilution (v/v)	5%	5%	25%	25%	50%	50%	50%
Wattage ($HRAP_2$)	450	450	450	900	900	1500	0
Dates	10/11/17-28/01/18	29/01/18-08/05/18	08/05/18-12/07/18	13/07/18-01/11/18	02/11/18-28/02/19	01/03/19-08/05/19	09/05/19-18/06/19
Elapsed time (d)	79	99	65	77	119	59	49
Average of daily max. Sunlight PAR ($\mu mol \cdot m^{-2}\ s^{-1}$)	3144±803	3661±753	2989±535	3572±359	3953±360	3629±352	3056±677
Ambient T(°C)	24±2	22±2	20±1	21±2	24±2	23±1	20±1
Daylight hours (h)	14±1	13±1	12±0	12±1	14±1	12±1	12±1
Total rainfall (mm)	564	723	12	851	277	247	29
No. of feedings	47	80	46	77	72	41	35
Digestate flow rate ($L \cdot d^{-1}$)	95	111	92	78	76	87	89
HRT_a (d)	13.2	10.7	13.6	16	16.4	14.4	14

The effluent flow rate (Q_e) of each system was estimated considering evaporation rates and volumes of wasted biomass. Evaporation rates were measured by daily assessing the depth levels in each HRAP. Biomass wastage was calculated aiming at maintaining a solid residence time (SRT) of 18 d and carried out directly for each pond to maintain the selected SRT based on volatile suspended solids concentrations. Environmental conditions were assessed based on ambient temperature, sunlight and rainfall. Values of pH, dissolved oxygen (DO) concentrations, and temperature were measured directly in the HRAPs, settler effluent and recycled biomass twice a week. Samples for physicochemical and microbiological analyses were collected once a week from the influents (*In*), HRAPs (*H*), effluents (*e*) and recirculation lines (R). Concentrations of total and soluble chemical oxygen demand (COD, sCOD), total and volatile suspended solids (TSS, VSS), total Kjeldahl nitrogen (TKN), total ammonia nitrogen (TAN), organic nitrogen (N-Org), and inorganic oxidized nitrogen (N_{NO}) estimated as the sum of nitrite-N and nitrate-N, were measured. Total alkalinity, total phosphorus (TP) and microalgae population structure were also weekly assessed. A triplicate of samples collected weekly from both HRAPs was fixed in paraformaldehyde and used to quantify the percentage of

167 photosynthetic organisms through flow cytometry analyses at the end of each stage. Similarly,
168 samples from digestate were collected in triplicate for assessing C, N and P concentrations in the
169 solid fraction.

170 **2.4 Analytical procedures**

171 Temperature, solar radiation and rainfall data were collected from a nearby meteorological
172 station (19°88'39.45" S; 43º96'93.97" W) operated by the Brazilian National Institute of
173 Meteorology. The average maximum daily values of solar radiation were transformed from
174 $W \cdot m^{-2}$ to photosynthetically active radiation (PAR) by applying a factor of 4.6. Light intensities
175 in the cultivation broths were measured using a PAR sensor SKL2623/I 43817 connected to a
176 data logger Datahog2® (SKYE INSTRUMENTS®). pH was determined using a benchtop pH-
177 meter (Denver Instruments® UB-5), whereas DO and T were measured electrochemically
178 (ALFAKIT AT170). COD, TAN, TKN, TSS, VSS, Total Alkalinity, and TP analyses were
179 carried out according to the Standard Methods for Water Examination (Rice *et al*., 2012).
180 Concentrations of organic nitrogen (OrgN) were obtained as the difference between TKN and
181 TAN. Soluble COD and nitrite-N + nitrate-N (N_{NO}) concentrations were assessed on properly
182 diluted samples filtered through membranes with a pore size of 0.45 µm. N_{NO} was measured
183 using NitraVer5® Nitrate Reagent Powder Pillows (HM 8039). Free ammonia nitrogen
184 concentrations (FAN) were calculated using the equations $FAN=TAN\left(1+10^{pK_a-pH}\right)^{-1}$; in which
185 pK_a is the dissociation constant for the ammonium ion as a function of temperature (T), $pK_a=$
186 $0.09018+2729.92(T+273.15)^{-1}$. Samples for elemental composition of the digestate (C, N and P
187 content) were lyophilized in a lyophilizer Liotop® L101 (Liobras, SP, Brazil). C and N content
188 was determined on a FLASH HT Plus elemental analyzer coupled to a Thermo Finnigan DELTA
189 Plus Advantage mass spectrometer (Thermo Electron Corporation, Waltham, MA, USA). Total

190 phosphorus (TP) of lyophilized samples was determined with standard spectrophotometric
191 methods, following persulfate digestion of samples (Rice *et al*., 2012).

192 Microalgae were identified using an optical microscope (Olympus CH30, Japan) and quantified
193 by the Utermöhl technique using an inverted microscope (Zeiss, Primovert – Germany). For
194 analyses of photosynthetic organisms by flow cytometry, samples were treated with Tween 80 to
195 break flocs structure' and fixed in paraformaldehyde before analyses (Eland *et al*. 2019). The
196 structure of photosynthetic organisms' population in both HRAPs was assessed through auto-
197 fluorescence using an APC-Cy7 laser in a BD LSRFortessa® cytometer. Paraformaldehyde and
198 samples of digestate and pure cultures of *Scenedesmus*, *Escherichia coli*, and *Pseudomonas* sp.
199 were used to configure gate properties during data analyses in the FLOWJO® software.

200 **2.5 Mass balances calculations**

201 Mass balances of TSS, COD, nitrogen compounds, and TP in $HRAP_1$ and $HRAP_2$ were
202 calculated using the measured concentrations and estimated flow rates. Removal efficiencies,
203 biomass productivities, nitrogen volatilization, nutrient recoveries and energy consumption
204 factors were estimated according to equations S.1 to S.13 (Supplementary material).

205 **2.6 Light intensity calculations**

206 Beer-Lambert´s law ($I_{(z)} = I_{(a)}\, e^{-K_d Z}$) was used to analyze light attenuation in the ponds.
207 Attenuation coefficients for downward irradiance (K_d) were estimated by linearization of PAR
208 profiles for both solar and LED lighting, using the Solver function in Microsoft Excel®,
209 minimizing the sum of the squared errors. The total light experienced by a cell moving up and
210 down through the water column per day (E_{mix}) for each pond was calculated as suggested by
211 Sutherland *et al.* (2014) ($E_{mix} = \left((1\text{-}e^{K_d Z_{mix}})\ (K_d Z_{mix})^{-1} \times \text{daily surface irradiance}\right)$, where Z_{mix} is

212 the HRAP depth. For $HRAP_1$, Z_{mix} corresponded to 0.3 m. In the $HRAP_2$, E_{mix} (*total*) was
213 estimated as the sum of E_{mix} (*LED*) and E_{mix} (*Sunlight*), each calculated using the attenuation
214 coefficients estimated for LED light and sunlight. Z_{mix} (*LED*) was the channel width (0.3 m),
215 whereas Z_{mix} (*Sunlight*) was the depth of $HRAP_2$ (1.2 m). The *Daily surface irradiance*
216 corresponded to the PAR intensity (*Sunlight* or *LED*) multiplied by the surface area of each pond
217 (*Sunlight*) or the total area of LED panels (*LED*). Profiles of sunlight and LED PAR intensities in
218 the HRAPs were measured on three different days at the end of each operational stage, using the
219 PAR sensor.

220 **2.7 Statistical analyses**

221 Two-way repeated-measures ANOVA was used to compare data from both ponds, operational
222 conditions and their interaction, for the variables describing the environmental conditions (T, pH,
223 PAR), and the treatment performance in the HRAPs (removal efficiencies of COD, TKN, TAN
224 and TP). Each HRAP was considered the main effect (F_H) and stages as within-subject variables
225 (F_S). A significance level of 0.05 was adopted for these analyses. Data were $\log_{10}(x+1)$ converted
226 prior to analysis. Normality was assessed using the Shapiro-Wilk test, homoscedasticity was
227 checked with Mauchly's Test of Sphericity, and the Greenhouse–Geiser df correction was used
228 for autocorrelation when necessary. When significant differences were proven, a Bonferroni's
229 pairwise comparison was carried out. A principal component analysis (PCA) was performed for
230 the main variables describing treatment performance and environmental parameters in the
231 HRAPs. The main variables were defined as the minimum number of variables producing the
232 highest percentage of explained variance in the PCA's first two components, using a stepwise
233 selection approach. Data were log10(x+1) transformed to homogenize measurement scales. The
234 data's adequacy for the PCA was verified using the Kaiser-Meyer-Olkin (KMO) Measure of

Sampling Adequacy for the overall data set. The suitability for data reduction was detected using Bartlett's test of sphericity. The PCA results were interpreted by analyzing the correlation coefficients and significance of the main components and the components plot, and by multiple linear regression using log-transformed variables showing significant effects (F-test, $p<0.05$) on COD, TAN and TKN removals (RE-COD, RE-TAN and RE-TKN). The selection of variables for the final models was made using backward elimination. Regressions models included the continuous predictor variables (*i*) T, E_{mix}, and the ratio $\frac{g\ N_{NO}}{g\ COD\ d^{-1}}$ for RE-COD, (*ii*) The percentage of influent alkalinity consumed in the HRAPs (Alk(%)), T, and E_{mix} for RE-TAN, and (*iii*) RE-TAN and N_{LOST} for RE-TKN, as well as the type of reactor as a categorical dummy variable with the values 0 and 1 for the two reactor types (Cohen & Cohen, 1983). All regressions parameters presented significant effect (t-test, $p<0.05$). All analyses were conducted using SPSS®.

3 Results and discussion

3.1 Food waste digestate

The food waste digestate was characterized by high C, N, and P concentrations, mainly at 25% and 50%-digestate (Table 2), whereas concentrations of 5% were more similar to municipal wastewater. Carbon and nutrient concentrations were highly variable due to changes in food waste composition and to modifications in the operation of the anaerobic digester (Tampio *et al*. 2015; Vaneeckhaute *et al*., 2016). Based on total COD, TKN and TP, the mean C:N ratio was 4:1, whereas the N:P ratio ranged from 6:1 to 17:1. Similar ratios reported for food waste digestates (Chuka-Ogwude *et al*., 2020) confirmed the high N availability compared to microalgae requirements (C:N of ~6:1 and N:P of ~7:1) (Benemann, 2003). The influent

digestate contained a high fraction of OrgN (23-33%) since negligible N transformation occurred during the anaerobic digestion of food waste in stages before the HRAPs. The sCOD corresponded to 5% to 55% of the total COD, suggesting that most of the organic carbon presented low biodegradability. Alkalinity, used as a proxy of the CO_2 available for photosynthesis, was mainly produced by the dissolution of CO_2 released during anaerobic digestion (Gerardi, 2003).

Table 2 – Food waste digestate characterization (Mean ± S.D. (Coefficient of variation))

Parameter	Unit	Digestate concentration		
		5%	25%	50%
pH		6.7-8.4	6.8-8.9	7.7-8.9
TSS	$mg \cdot L^{-1}$	90±75 (83%)	359±139 (38%)	705±253 (36%)
COD	$mg \cdot L^{-1}$	238±121 (51%)	557±165 (29%)	1031±120 (12%)
sCOD	$mg \cdot L^{-1}$	14±11 (77%)	145±103 (71%)	364±218 (60%)
Total Alkalinity	$mgCaCO_3 \cdot L^{-1}$	248±137 (55%)	689±174 (25%)	1513±734 (46%)
Org-N	$mg \cdot L^{-1}$	11±10 (90%)	53±42 (79%)	138±108 (78%)
TAN	$mg \cdot L^{-1}$	36±21(57%)	135±43 (32%)	291±97 (33%)
TKN	$mg \cdot L^{-1}$	47±21(45%)	185±66 (35%)	418±161 (38%)
N_{NO}	$mg \cdot L^{-1}$	8±8 (99%)	7±8 (121%)	12±6 (51%)
TP	$mg \cdot L^{-1}$	10± (67%)	17±9 (55%)	28±8 (29%)
PO_4-P	$mg \cdot L^{-1}$	7±6 (90%)	10±7 (76%)	16±8 (49%)
C*	(%)	35±2	45±3	49±3
N*	(%)	8±3	5±1	6±1
P*	(%)	2.2±1.5	0.7±0.2	0.7±0.1

(*) Measured on a dry matter basis

3.2 Environmental parameters

The variations in the number of sunlight hours, natural PAR, and temperature, typical for the region, were characterized by hot rainy summers, colder dry winters and a low temperature amplitude (20-26°C), which provided adequate conditions for microalgal growth (Table 1) (Singh & Singh, 2015). Cultivation broth temperatures were significantly lower in both HRAPs during winter (S-II, S-III and S-VI, Table 3) (Pairwise comparison, $p<0.05$) and $HRAP_1$ was

271 warmer than $HRAP_2$ (except during S-III, S-VI and S-V) due to its larger area exposed to
272 sunlight and its shallow depth, which limited the attenuation of seasonal variations (Sutherland *et*
273 *al*., 2014). Conversely, the smaller surface area and higher depth of $HRAP_2$ resulted in better
274 temperature control and a reduction of evaporation rates by 20 to 90% (<1 to 1.7 $L \cdot m^{-2} \cdot d^{-1}$, Table
275 3) compared to $HRAP_1$. $HRAP_2$ was also less impacted by rainfall, while $HRAP_1$ experienced
276 high and instantaneous effluent flow rates and partial biomass wash-out during rainy days (a
277 typical limitation of HRAPs) (Nwoba *et al*., 2016). Additionally, the days without feedings
278 (Table 1) resulted in actual HRTs ranging from 10 to 16 d, which were longer than the nominal
279 value of 10 d and longer than recommended values (Anbalagan *et al*., 2016) but provided no
280 restriction for microalgae growth.

281 Increased pH, high DO concentrations and alkalinity consumptions (Table 3) were associated
282 with autotrophic microalgae activity. Digestate alkalinity supplied CO_2 for autotrophs in the
283 form of bicarbonate and provided buffer capacity that attenuated the variations in pH in both
284 HRAPs (Goldman *et al*., 1982). Higher mean DO concentrations occurred during S-I ($HRAP_1$:
285 15±4 $mg \cdot L^{-1}$, $HRAP_2$: 7±1 $mg \cdot L^{-1}$), but the higher digestate loads during the following stages
286 resulted in lower DO in both HRAPs (Table 3). $HRAP_1$ presented a more positive balance
287 between photo-aeration and DO consumption since higher DO levels, compared to $HRAP_2$, were
288 recorded throughout all the stages (pairwise comparisons, $p>0.05$). Mechanical mixing (paddle
289 wheels occupied ~ 40% of the HRAP area) may have slightly contributed to aeration in $HRAP_2$,
290 which was negligible in $HRAP_1$ (García *et al*., 2006). Thus, DO was mainly produced via
291 microalgae photosynthesis, whereas respiration, biodegradable organic matter oxidation and
292 nitrification were the main mechanisms responsible for DO consumption.

293 The pH was slightly alkaline in S-0 and S-I and relatively neutral in both HRAPs during the next
294 stages (Table 3). pH was positively correlated with DO (r_s= 0.56, $p<0.05$) and negatively
295 correlated with alkalinity consumption (r_s=-0.97, $p<0.05$) in $HRAP_1$, evidencing a strong
296 influence of autotrophic activity. The lower alkalinity consumptions occurred concomitantly
297 with higher pH values during S-0 and S-I (55±23% and 67±19%, respectively). This suggested a
298 potential CO_2 limitation for microalgae triggered by the displacement of the equilibrium of
299 bicarbonate to carbonate, which is not a carbon source for microalgae (De Godos *et al*., 2016).
300 The increase in bicarbonate load to $HRAP_1$ at digestate dilutions of 25% and 50% allowed
301 process operation at more neutral pH conditions. On the other hand, the pH in $HRAP_2$ remained
302 more neutral than in $HRAP_1$ due to the lower CO_2 consumption and thus higher buffer capacity
303 derived from digestate alkalinity. No significant correlations between pH and DO (Table 3) were
304 observed, although higher alkalinity consumptions and DO concentrations during S-0 and S-I
305 indicated a more intense autotrophic activity. The decrease in alkalinity consumption at a
306 digestate dilution of 25% (from 85% to 40% in S-I and S-II, respectively) was likely caused by a
307 hindered light penetration (PAR and E_{mix}, Table 3), which was partially mitigated by the
308 additional increase in the power of LED supplied to $HRAP_2$ during S-III. When digestate was fed
309 at 50% dilution, alkalinity consumption remained low, suggesting limiting conditions to
310 autotrophic activity, even when increasing the lighting power during S-V. Nutrients and
311 inorganic carbon availability from the digestate also suggested that these factors did not limit
312 $HRAP_2$ and light penetration may have been the main constrain for microalgae in this unit.

313 **3.3 Biomass concentration, settleability, and growth**

314 Higher VSS mean values were recorded in S-I, S-IV and S-V in $HRAP_1$ (163±51, 741±276 and
315 1178±267 $mg \cdot L^{-1}$, respectively) compared to $HRAP_2$ (60±10, 691±330 and 994±59 $mg \cdot L^{-1}$,

316 respectively), with $HRAP_2$ exhibiting similar VSS to $HRAP_1$ during all stages, (pairwise
317 comparisons, $p< 0.05$) (Fig. 2a, 2b). Overall, VSS concentrations in the HRAPs increased with
318 influent digestate concentrations due to higher biomass growth at higher nutrient loads. VSS in
319 the recirculation lines reached high average concentrations of up to 9.5 and 5.4 $gVSS \cdot L^{-1}$,
320 corresponding to 5 and 2-fold the VSS in $HRAP_1$ (S-VI) and $HRAP_2$ (S-V), preventing wash-
321 outs and contributing to maintaining adequate VSS concentrations in the HRAPs. The low
322 biomass wastage rates from both systems resulted in a low food to microorganism ratio (F:M,
323 based on influent COD), high SRT (~18 d) and low productivities in both HRAPs (negligible
324 during S-V and S-VI in both systems) (Table 3) (Eq. S.6- Supplementary Material), which also
325 decreased with increasing influent digestate concentration. The low F:M promoted a high contact
326 time between the biomass and the digestate, thus favoring the biodegradation of the recalcitrant
327 influent COD and supporting a high endogenous metabolism (Cagnetta *et al*., 2019). The growth
328 of microalgae and bacteria supported the increases in VSS in both HRAPs, which were
329 dominated mainly by chlorophytes, which are typically found in conventional stabilization
330 ponds, HRAPs, and other photobioreactor configurations for treating high-strength wastewaters
331 under indoor and outdoor conditions (Yan *et al*., 2015, Nwoba *et al*., 2016, Ayre *et al*., 2017;
332 Eland *et al*., 2018). In $HRAP_1$, the mean microalgae densities ranged from 10^9 to 10^{10} cell·g TSS^{-1}
333 and in $HRAP_2$ from 4×10^7 to 8×10^9 cell·g TSS^{-1}, with higher densities during S-0, S-I and S-II
334 (pairwise comparison). These densities observed in both HRAPs, mainly during S-0 and S-I,
335 were relatively similar to those observed in conventional HRAPs treating high-strength
336 wastewater (e.g., 0.3×10^7 to 3×10^7, Ayre *et al*., Torres-Franco *et al*., 2018). *Chlorella* sp. was
337 dominant in $HRAP_1$ during S-0, *Scenedesmus* sp. during S-I and S-II, whereas *Dyctiosphaerium*
338 sp, which showed higher efficiency in bicarbonate assimilation compared to other species (Qilu
339 *et al*, 2018), dominated the microalgae community in the next stages. This species was also the

most abundant in $HRAP_2$ during all stages, except in S-III, when *Stigeoclonium* sp., *Euglena* sp., and *Gomphonema* sp. were dominant. The predominance of Chlorophyta occurred likely as a consequence of the relatively high FAN concentrations recorded in both HRAPs (averaging 0.3-1.3 and 0-15.3 mg $NH_3 \cdot L^{-1}$ –$HRAP_1$ and $HRAP_2$, respectively), since this phylum is more tolerant to NH_3 (Collos & Harrison, 2014).

The dominances of *Scenedesmus* sp. and *Dyctiosphaerium* sp. during S-0 to S-II coincided with the highest shares of photosynthetic organisms measured by flow cytometry (Fig. 2c), revealing a higher density of phototrophs in $HRAP_1$ (8-55%) compared to $HRAP_2$ (1-30%). During S-IV to S-VI, the share of photosynthetic cells in $HRAP_1$ remained above 10% but dropped to values ranging from 0.5% to 5% in $HRAP_2$, which were similar to those observed in facultative ponds (Eland *et al*., 2018). Indeed, the supply of 50%-digestate resulted in severe light attenuation in $HRAP_2$, significantly reducing microalgae densities. Flow cytometry revealed that the increase in LED power during S-III contributed to overcoming the light limitation in the cultivation broth, thus slightly increasing photosynthetic organism percentages compared to S-II (2.2 and 4.3%, respectively) with significant drops in microalgae densities, which was likely mediated by the development of a mixotrophic microalgae community. Thus, mixotrophic microalgae well-adapted to low light availability such as *Stigeoclonium* sp., *Euglena* sp., and *Gomphonema* sp. emerged during S-III. *Euglena* is a common genus in HRAPs, which can grow under mixotrophic conditions (Yamane *et al*., 2001, Mahapatra *et al*., 2013) at low light intensities and high concentrations of organic matter. Similarly, the mixotrophic metabolism of *Gomphonema* sp. (Marella *et al*., 2018) and *Dyctiosphaerium* sp. (Ogbonna *et al*., 2018) supported their dominance from S-IV to S-VI. Finally, *Stigeoclonium* sp. can grow in light-limited environments such as the inner layers of microalgal-bacterial biofilms (Kim *et al*., 2015).

Table 3 – Environmental parameters in the HRAPs, food to microorganism ratio (F:M), sludge retention time (SRT), biomass productivities, influent concentrations ($mg \cdot L^{-1}$), removal efficiencies of TSS, and COD, nitrogen forms (TKN, TAN, N_{NO}), and TP, nitrogen losses (N_{LOST}), and nitrogen assimilated (N_A) (Mean±S.D.) for $HRAP_1$ and $HRAP_2$ during the operational stages tested.

Parameter	Stage (Digestate dilution, v/v)													
	0 (5%)		I (5%)		II (25%)		III (25%)		IV (50%)		V (50%)		VI (50%)	
	$HRAP_1$	$HRAP_2$	$HRAP_1$	$HRAP_2$	$HRAP_1$	$HRAP_2$	$HRAP_1$	$HRAP_2$	$HRAP_1$	$HRAP_2$	$HRAP_1$	$HRAP_2$	$HRAP_1$	$HRAP_2$
T (°C)	26±3	25±2	26±3	24±2	21±1	20±1	24±3	23±2	26±3	25±2	26±2	25±2	21±1	20±1
DO ($mg \cdot L^{-1}$)	15±3	8±3	15±4	7±1	11±4	1±1	10±3	1±1	6±4	1±1	3±2	0.5±0.4	3±2	0.4±0.1
pH	8.1-9.9	5.9-9.2	7.6-10.4	5.8-7.7	6.3-8.6	7.9-7.4	6.0-8.3	7.2-8.0	5.8-8.3	7.2-8.9	6.2-7.7	8.0-8.4	7.1-7.7	7.8-8.5
Alkalinity Consumption ($g\ CaCO_3 \cdot d^{-1}$)**	18±11 (55±23%)	57±33 (84±15%)	30±19 (67±19%)	35±16 (85±10%)	100±30 (82±6%)	45±24 (40±17%)	59±14 (90±7%)	54±20 (74±13%)	221±114 (94±3%)	172±99 (71±16%)	114±48 (95±2%)	95±50 (58±18%)	97±50 (88±9%)	45±33 (50±22%)
Evaporation rate ($L \cdot m^{-2} \cdot d^{-1}$)	3.9±8.3	2.4±4.0	6.5±3.5	1.7±3.0	4.9±6.8	4.1±7.9	7.8±7.2	0.8±2.4	7.1±10.9	1.3±2.5	5.5±6.1	<1.0	6.1±7.5	1.7±3.7
Sunlight PAR ($\mu mol \cdot m^{-2} \cdot s^{-1}$)	681±187	387±170	535±477	359±218	360±185	352±327	677±357	678±378	420±40	321±173	444±244	225±64	185±123	173±58
E_{mix} (*total*)($mol \cdot d^{-1}$)	28±10	13±3	13±2	7±2	6±1	0.5±0.1	7±2	0.5±0.1	8±3	0.4±0.1	5±1	0.3±0.1	4±1	0.3±0.3
F:M ($g\ COD \cdot g\ VSS^{-1}\ d^{-1}$)	0.15	0.41	0.07	0.29	0.13	0.16	0.07	0.21	0.15	0.15	0.04	0.04	0.07	0.04
SRT (d)	-	-	12±6	13±5	16±5	20±9	21±2	17±5	19±5	21±6	20±2	18±3	24±5	19±2
Productivity ($gVSS \cdot m^{-2} d^{-1}$)	9±6	3±2	9±7	3±3	5±7	2±3	2±4	6±5	6±8	4±10	0	0	0	0
TSS In ($mg \cdot L^{-1}$)	121±96	108±98	88±67	66±39	385±109	345±129	276±105	351±159	802±230	875±309	593±136	769±220	651±92	594±52
RE –TSS (%)	61±36	58±31	23±32	46±36	74±10	74±9	48±11	54±18	72±10	69±15	57±11	62±11	71±24	57±13
COD In ($mg \cdot L^{-1}$)	212±166	231±40	185±94	183±92	549±113	490±108	571±184	609±188	1066±90	1074±103	1021±80	1058±93	928±134	924±162
RE-COD (%)	67±23	74±16	59±10	76±23	62±22	71±15	50±12	52±9	58±15	39±16	55±15	39±11	74±16	48±13
TKN In ($mg \cdot L^{-1}$)	46±16	40±19	49±21	51±29	204±68	203±57	138±47	165±56	463±204	462±188	410±149	431±133	353±53	333±55
RE-TKN (%)	79±5	66±20	48±16	67±12	65±20	42±33	62±16	50±20	86±12	64±20	87±8	55±16	69±37	24±21
TAN In ($mg \cdot L^{-1}$)	34±19	34±23	38±21	39±17	148±36	144±34	107±42	124±54	328±135	342±121	274±31	266±45	224±37	250±58
RE-TAN (%)	75±23	80±4	79±6	81±5	70±16	44±25	75±13	63±24	90±12	66±22	94±3	53±20	75±32	30±9
$N_{lost\ (\%)}$	75±7	68±22	41±24	42±17	41±32	31±29	25±23	37±35	60±20	48±26	63±10	32±22	51±31	7±12
$N_{A\ (\%)}$	4±6	4±3	16±11	5±6	3±5	4±7	7±12	7±11	1±2	4±8	3±6	1±3	6±13	22±23
TP In ($mg \cdot L^{-1}$)	15±10	17±10	7±4	8±6	26±9	23±7	11±6	12±4	31±9	31±8	28±7	26±6	24±8	24±5
RE-TP (%)	39±19	62±44	31±28	23±16	52±18	40±21	16±22	19±29	57±14	34±22	59±12	33±25	42±28	21±18
Energy consumption factor ($kWh \cdot m^{-2}$)($kWh \cdot d^{-1}$)	0.36 (1.6)	2.88 (4.0)	0.36 (1.6)	2.88 (3.7)	0.36 (1.6)	2.88 (3.7)	0.36 (1.6)	4.26 (5.2)	0.36 (1.6)	4.26 (5.2)	0.36 (1.6)	5.64 (7.0)	0.36 (1.6)	1.6 (1.6)
LED power $HRAP_2$ (W)	450		450		450		900		900		1500		0	

T: $F_{O.C}$= 39.440; F_H =68.415*; F= 3.650*; DO: $F_{O.C}$= 7.351*; F_H =12.161*; F= 9.521*; pH: $F_{O.C}$= 4.456*; F_H =0.002*; F= 8.586*; Alk: $F_{O.C}$= 0.822; F_H =4.61*; F= 3.878*; TSS: $F_{O.C}$= 18.422*; F_H =0.461; F= 1.376; RE –TSS: $F_{O.C}$= 2.595; F_H =1.549; F= 2.033; COD In: $F_{O.C}$= 82.258*; F_H = 0.852; F= 3.448; RE-COD: $F_{O.C}$=4.744*; F_H =0.308; F= 2.330; RE-TKN: $F_{O.C}$=1.865*; F_H =16.867*; F= 5.600*; RE-TAN: $F_{O.C}$=4.920*; F_H =37.828*; F= 5.431*; RE-TP: $F_{O.C}$=2.486; F_H =26.274*; F= 0.624*

3.4 TSS and COD removal

Both HRAPs supported an adequate solids separation as a result of the good settleability of the microalgal-bacterial biomass of both HRAPs, as confirmed by the SVI (Fig. 2d). Overall, the SVI increased with digestate load. Average SVI ranged from 22 to 89 $mL \cdot g^{-1}$ in $HRAP_1$ and from 2 to 137 $mL \cdot g^{-1}$ in $HRAP_2$. An SVI in the range of 40-120 $mL \cdot g^{-1}$ typically entails an overall good performance in TSS removal (Table 3), similar to the observations of Hende *et al*. (2011). Fig. 3a shows the influent and effluent TSS concentrations in both HRAPs. Average TSS removal efficiencies varied from 23±32% (S-I) to 74±10% (S-II) in $HRAP_1$ and from 46±36% (S-I) to 74±9% in $HRAP_2$ (S-II). No significant differences were observed along the different operational stages or between HRAPs (Pairwise comparisons, Table 3). Higher efficiencies were not reached likely due to the limited hydrodynamic performance of the settlers (operated at long HRTs and under semi-continuous mode).

COD removal efficiencies ranged from 50±12% (S-III) to 74±16% (S-VI) in $HRAP_1$ and from 39±16% (S-IV) to 76±23% (S-I) in $HRAP_2$. $HRAP_2$ matched the performance of $HRAP_1$ for all stages except S-I and S-VI, where significantly higher and lower efficiencies were achieved, respectively. $HRAP_2$ supported significantly lower COD removal efficiencies from S-IV to S-VI than those recorded in previous stages (pairwise comparison, $p>0.05$) due to the reduced photo-aeration capacity of microalgae in this unit when treating 50%-digestate. Overall, the low F:M ratios, long SRT of operation and favorable temperature and solar radiation favored the biological oxidation of the recalcitrant COD in both HRAPs. The COD removal efficiencies here reported were similar

391 or even higher than values obtained in similar studies in the literature (*e.g.,* 35%-38% in

392 Garcia *et al*., 2006, 48%-76% in De Godos *et al*., 2009).

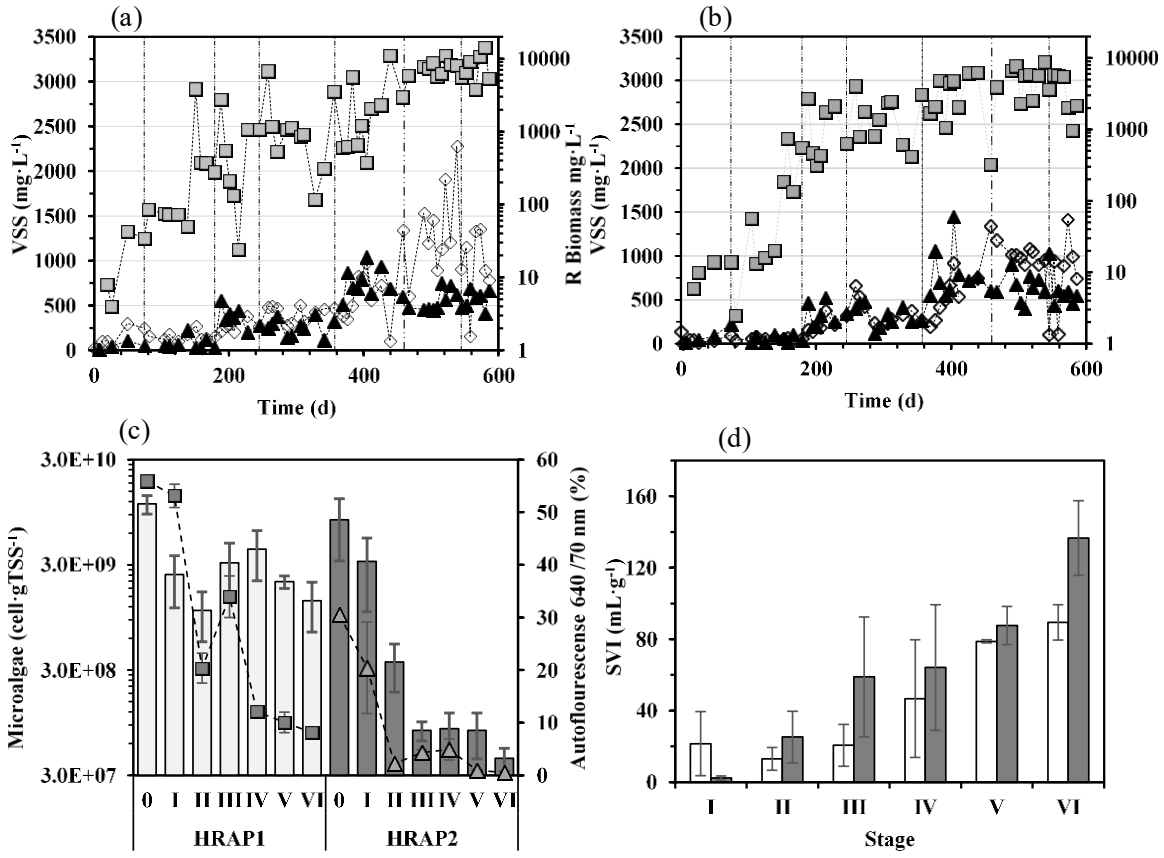

393

394 **Figure 2** –VSS concentrations in the influent (▲), HRAP (◊), and Recycled-R stream (■)
395 in (a) $HRAP_1$ and (b) $HRAP_2$ (significant differences within stages, F_S=50.749, and
396 between HRAPs, F_H= 35.160). (c) Densities of microalgae per gram of VSS in $HRAP_1$
397 (blank) and $HRAP_2$ (gray) (Significant differences within stages, F_S=26.731, and between
398 HRAPs, F_H= 167.988) and percentages of photosynthetic organisms (autofluorescence 640
399 /70 nm) for (■) $HRAP_1$ and (▲) $HRAP_2$ (secondary axis); and (d) bar chart of the sludge
400 volumetric index (SVI) of biomass produced in $HRAP_1$ (gray filled) and $HRAP_2$ (blank).

401 **3.5 Nitrogen and phosphorus transformations and removal**

402 TAN removal efficiencies ranged from 70±16% (S-II) to 94±3% (S-IV) in $HRAP_1$, whereas
403 $HRAP_2$ provided TAN removals between 30±9% (S-VI) and 81±5% (S-II). $HRAP_2$
404 matched the performance of $HRAP_1$ in all stages, except in S-V and S-VI, where lower
405 efficiencies were achieved (Table 3). The removals of TKN ranged between 48±16% (S-II)

406 and 87±8% (S-V) in $HRAP_1$, and between 21±21% (VI) and 67±12% (II) in $HRAP_2$, which
407 matched $HRAP_1$ performance in S-I, S-III and S-IV, and achieved a higher performance in
408 S-II and lower efficiencies in S-V and S-VI. No significant differences within stages were
409 detected in TKN removal in both ponds (Table 3). TAN and TKN removal efficiencies
410 achieved in the $HRAP_s$ were comparable with those obtained by de Godos *et al*. (2009)
411 (TKN: 48-88%) in a similar system, but lower compared to systems with external CO_2
412 addition and no light limitations (e.g., TN-RE: 98%, Marin *et al*., 2018).

413 Ammonium nitrification-denitrification and volatilization as NH_3 or N_2 seemed to be the
414 main N removal pathways in both HRAPs. NH_3 stripping occurred as a result of the high
415 pH values prevailing in the cultivation broths, whereas N_2 was produced via nitrification-
416 denitrification under alternating oxic-anoxic conditions. $HRAP_1$ showed a trend to achieve
417 higher TAN and TKN removal when increasing N_{LOST} (Eq. S.4- Supplementary Material),
418 as confirmed by the positive correlations of this parameter with RE-TAN (r_s 0.64, $p<0.05$)
419 and RE-TKN (r_s 0.71; $p<0.05$). In the $HRAP_1$, the N_{LOST} varied between 25±23% (S-III)
420 and 75±7% (S-0). Thus, the $N_{LOST,}$ during S-0 and S-I was mainly caused by ammonia
421 volatilization as a result of the highly alkaline conditions and high FAN (mean FAN 67%
422 of $TAN_{(H)}$). NH_3 volatilization decreased due to the lower FAN at increasing digestate
423 dilutions, which decreased to 1-3% of the TAN in the culture broth ($TAN_{(H)}$) during S-II
424 and S-III and to less than 1% from S-IV to S-VI. Process operation at higher digestate loads
425 entailed higher CO_2 and TAN available for nitrification. Indeed, the highest N_{NO} measured
426 in the $HRAP_1$ was 69±84 $mg \cdot L^{-1}$ during S-IV. The negative correlation observed between
427 $TAN_{(H)}$ and DO (r_s= -0.61, $p<0.05$) supports the occurrence of nitrification, mainly during
428 S-II to S-VI (where more neutral pH conditions prevailed) (Buchanan *et al*. 2018).

Denitrification was also favored under the high organic carbon loads and more neutral pH conditions prevailing from S-II to S-IV, and the low DO concentrations during nighttime (Plouviez *et al*., 2019). However, the availability of easily biodegradable organic carbon and nitrite likely limited the denitrification in the $HRAP_1$ (Alcántara *et al*., 2015), thus preventing higher TKN removal.

In $HRAP_2$, TAN and TKN removal were also positively correlated with N_{LOST} (r_s 0.59 and 0.81, $p<0.05$, respectively), suggesting that volatilization played a major role in N removal in this unit, mainly during process operation with 5% and 25%-digestate. Nitrogen was volatilized mainly by NH_3 stripping or N_2 produced by nitrification-denitrification, which are the processes typically responsible for N-volatilization in HRAPs treating digestate (De Godos *et al*., 2016). Despite the slightly neutral pH during all the operational stages, approximately 10% of FAN was recorded in the cultivation broth of $HRAP_2$ (Table S.10 – Supplementary material), fostering ammonia stripping. Nitrification occurrence was evidenced by the production of N_{NO} (Table 3), even at the low DO concentrations recorded, as previously reported by How *et al*. (2019). The maximum N_{NO} concentration achieved in $HRAP_2$ was 59±40 $mg \cdot L^{-1}$ (S-II). N_{NO} concentrations in $HRAP_2$ were similar to those recorded in $HRAP_1$ during S-0, S-I and S-III, but lower during the other stages. On the other hand, denitrification in $HRAP_2$ occurred at low DO concentrations during nighttime in S-0 and S-I and was favored in further stages due to the low DO values in $HRAP_2$. The environmental and operational conditions during S-II and S-III may have favored partial simultaneous nitrification-denitrification, since mean DO values were always low but higher than 0.2 $mg \cdot L^{-1}$, which has been suggested as a minimum value for nitrification (Jia *et al*., 2016) allowing denitrification in the inner parts of the flocs (Bai *et al*., 2016).

Furthermore, N_2O volatilization possibly occurred in $HRAP_2$ promoted by low DO concentrations (Plouviez *et al*., 2019).

Nitrification-denitrification or nitrogen removal pathways other than ammonia volatilization (*i.e*., assimilation) are desirable since free ammonia is a precursor of greenhouse gases (Alcántara *et al*., 2015). Furthermore, removing ammonium is desirable to prevent reactor´s acidification derived from high concentrations in the absence of buffering capacity (Nakamura *et al*., 2017). Assimilation was the second most important mechanism of removal, mainly in the stages with lower values of N_{Lost} (I to III in $HRAP_1$ and in $HRAP_2$ during all the Stages). The low C:N ratio of the digestate and the absence of CO_2 addition prevented higher N assimilation, limiting the achievement of higher removals in both HRAPs. Similar to Arcila & Buitron (2016) and Rada-Ariza *et al*. (2019), the low rates of assimilation were related to the long HRT and SRT promoted by the high VSS in the HRAPs and the low biomass wastage rates, which prevented exponential microalgal growth. The actual extent of N assimilation remained unaccounted for since a high fraction of OrgN:TKN in the influent digestate (0.3 for all digestate concentrations) was permanently measured, suggesting that assimilation rather represented a transformation of the influent organic forms into microalgal-bacterial biomass than a net transformation of mineral nitrogen into organic nitrogen.

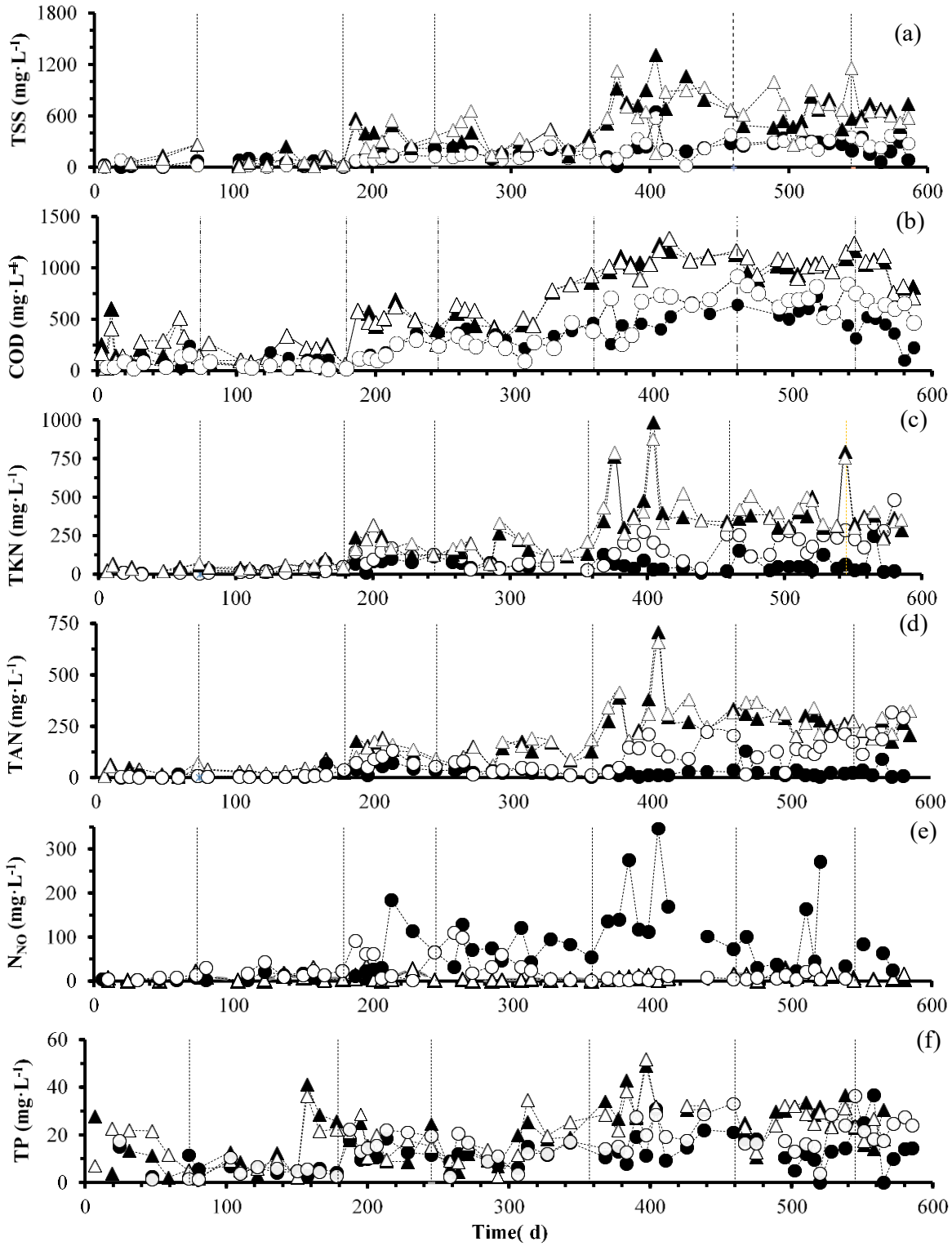

Figure 3 – Time course of (a) TSS; (b) COD; (c) TKN; (d) TAN; (e) N_{NO} and (f) TP concentrations in the influent of $HRAP_1$ (▲) and $HRAP_2$ (△), and effluent of $HRAP_1$ (●) and $HRAP_2$ (○)

TP was removed with mean efficiencies ranging from 25 to 76% in $HRAP_1$ and from 22 to 63% in $HRAP_2$. No differences were detected within stages neither for $HRAP_1$ nor $HRAP_2$. Furthermore, the pairwise comparison showed that $HRAP_2$ match the performance of $HRAP_1$, except in S-0, S-I and S-III. Similar values were obtained for soluble phosphorus (Table S.8-Supplementary Material). Assimilation into microalgal-bacterial biomass (Posadas *et al*., 2014) and separation of biomass in the settler removing P bound to organic matter from the effluent were likely the main mechanisms of phosphorus removal. No P depletion occurred in both HRAPs, suggesting that this nutrient was not limiting for microalgae growth and supporting the hypothesis that CO_2 and light were the main limiting factors in $HRAP_1$ and $HRAP_2$, respectively.

3.6 Influence of LED-enhancement on carbon and nitrogen transformations

In $HRAP_1$, high DO and pH values occurred under lower influent digestate load, as indicated by the first component (PC1, 42.7%) of the PCA (Fig. 4a). Samples from S-0 and S-I (5% digestate) also entailed high negative scores in PC1, showing associations with high values of pH, DO and E_{mix}. In contrast, some samples from S-II and S-III (25%) and all from S-IV to S-V (50%) exhibited positive scores in PC1, stressing that the increase of influent digestate concentrations decreased light intensity (E_{mix}) in the unit and entailed a higher oxygen demand for organic carbon and N transformation and removal, resulting in lower pH and DO in the $HRAP_1$. On the other hand, the second component (PC2, 18.5%) showed associations between microalgae growth and treatment performance. In this component, E_{mix}, pH, DO, microalgae densities (cell·TSS^{-1}) and treatment efficiencies (including N_{LOST}) showed associations, suggesting a positive effect of high microalgae densities on treatment performance. High availability of light and nutrients, and mild

497 temperatures under more neutral pH, mediated by higher influent alkalinity due to the use
498 of 25% and 50%-diluted digestate favored microalgae growth, as suggested by the
499 associations between these variables and microalgae density. Samples positively correlated
500 with PC2 were related to lower treatment performance, mainly during S-II and S-III, which
501 coincided with winter and autumn, and were likely affected by lower values of PAR and T.
502 In this context, Vassalle *et al*. (2020a and 2020b) observed that also low values of PAR
503 during the local rainy period of summer-fall may promote low performance and microalgae
504 densities (as also verified in the $HRAP_1$ by Spearman correlations: cell·TSS^{-1} –T $r_s = 0.37$,
505 and cell·TSS^{-1} –E_{mix} $r_s = 0.33$, $p<0.05$).

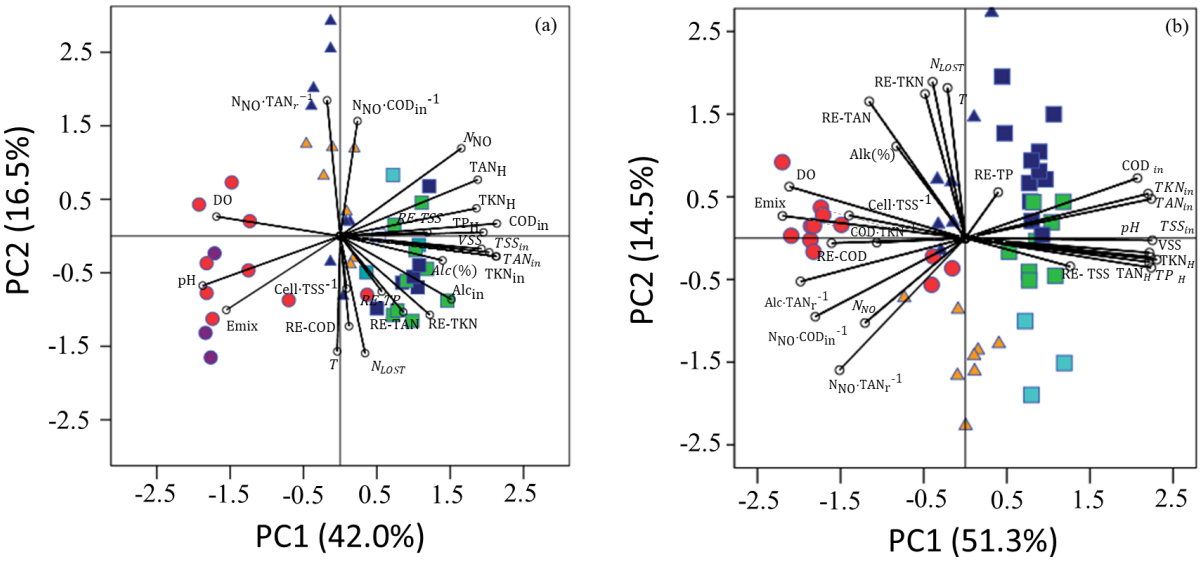

506

507 **Figure 4** – Principal component analysis (PCA) plot for the main variables of
508 nvironmental and biological conditions and treatment performance for (a) $HRAP_1$ and (b)
509 $HRAP_2$ during the treatment of 5% (●), 25% (▲) and 50% (■) digestate. S-0: purple circle;
510 S-I: red circle; S-II: blue triangle; S-III: orange triangle; S-IV: blue square; S-V: green
511 square; S-VI cyan square.

512 The PC1 of the PCA for $HRAP_2$ (46.1%) was positively correlated with digestate
513 composition (*i.e.,* $TSS_{(in)}$, $TKN_{(in)}$, $COD_{(in)}$) and the physicochemical characteristics of the
514 HRAP cultivation broth (*i.e.,* T, $TKN_{(H)}$, $N_{NO(H)}$, $VSS_{(H)}$) (Fig. 4b). Conversely to $HRAP_1$,

515 the pH and DO presented opposite correlations with the component. Additionally, E_{mix}, T,
516 DO, microalgae densities, RE-COD, RE-TAN, $N_{LOST,}$ and N_{NO} were negatively correlated
517 with PC1. This suggests that low solids concentrations in the $HRAP_2$ resulted in higher
518 light availability (E_{mix}) for microalgae growth, and thus higher DO from the microalgal
519 activity. The positive correlation between pH and the PC1 indicated that digestate
520 composition, rather than microalgal activity, controlled pH in $HRAP_2$. Furthermore, the
521 presence of microalgae boosted COD, TAN and TKN removals, whereas these variables
522 were negatively affected by the increase in digestate load. These trends were also
523 confirmed by the negative scores of S-0 and S-I samples with the PC1. Finally, the PC2
524 indicated associations of N_{Lost}, and TAN and TKN removals with E_{mix}, DO and microalgae
525 densities.

526 Multiple regression analyses (*i-iii; F-test,* $p<0.05$) confirmed the associations shown by the
527 PCA for both systems. Temperature, E_{mix} and the ratio between N_{NO} produced in the
528 HRAPs and influent COD ($\frac{g\ N_{NO}}{g\ COD\ d^{-1}}$) were the main variables explaining COD removal (*i*).
529 Optimum temperatures and higher E_{mix} (which considers light attenuation and availability
530 and HRAPs depth) entailed higher COD removals. High values of the $\frac{g\ N_{NO}}{g\ COD\ d^{-1}}$ ratio
531 indicated better conditions for denitrification. In $HRAP_1$, more intense nitrification
532 resulting in high N_{NO} production likely affected aerobic bacterial organic carbon
533 consumption due to DO consumption by nitrification, as indicated by the negative sign in
534 the equation for $\frac{g\ N_{NO}}{g\ COD\ d^{-1}}$, whereas in $HRAP_2$, the fraction of COD removed by anoxic
535 carbon consumption during denitrification was likely higher than the aerobic or
536 mixotrophic comsumption, as expressed by the positive sign of $\frac{g\ N_{NO}}{g\ COD\ d^{-1}}$ in the regression.

TAN removals (*ii*) were explained by the percentage of alkalinity consumed in the HRAPs, temperature and E_{mix}, whereas TKN removals (*iii*) were functions of TAN removal and N volatilization (N_{LOST}). Variables used in the regression explaining RE-TKN showed no effect derived from the type of reactor, resulting in a combined model for the two HRAPs. Relatively low R^2 values suggested that other variables than those measured in this study also affected the treatment performance in $HRAP_1$.

(*i*) $$\text{RE-COD}=\begin{cases}\text{HRAP}_1\text{: } 2.556-0.636T+0.112E_{mix}-1.874\left(\frac{g\ N_{NO}}{g\ COD\ d^{-1}}\right)\\ \text{HRAP}_2\text{: } 2.556-0.636T+0.112E_{mix}+1.653\left(\frac{g\ N_{NO}}{g\ COD\ d^{-1}}\right)\end{cases}$$ (R^2=0.50; F=7.320, p=0.00)

(*ii*) $$\text{RE-TAN}=\begin{cases}\text{HRAP}_1\text{: } 0.287+0.403Alk(\%)+0.600T-0.065E_{mix}\\ \text{HRAP}_2\text{: } 0.287+0.403Alk(\%)+0.600T-0.371E_{mix}\end{cases}$$ (R^2 =0.77; F=8.306, p=0.00)

(*iii*) $$\text{RE-TKN}= 0.953+0.356\text{RE-TAN}+0.14N_{LOST}$$ ($HRAP_1$/$HRAP_2$) (R^2 =0.80; F=67.602, p=0.00)

Although light limitation under high solids concentration in $HRAP_2$ resulted in a shift from microalgae-driven (S-0 to S-I) to bacteria-driven treatment processes (S-II to S-V), the LED-enhancement showed to be efficient in significantly reducing the conventional area of HRAPs. Successful applications in the treatment of high-strength digestates will depend on reducing influent TSS loads or on the economic feasibility of increasing LED power to overcome lighting limitations.

3.7 Treatment capacity, energy consumption and biomass valorization

Figure 5 shows the comparison of treatment performance and energy consumption between HRAPs. TSS removal in $HRAP_2$ and $HRAP_1$ were similar at all influent loads tested. Overall, $HRAP_1$ had mean COD removal efficiencies ranging from 58 to 75% at OLR 100 g $COD \cdot m^{-3} \cdot d^{-1}$ (S-IV to S-VI), confirming the potential of conventional HRAPs to treat high strength wastewater with highly recalcitrant influent COD. At low COD and N loads

(Fig. 5h 5i), $HRAP_2$ presented a similar treatment performance, although the data exhibited high variability. At higher loads (~75 g $COD \cdot m^{-3} \cdot d^{-1}$, 20 g $TAN \cdot m^{-3} \cdot d^{-1}$, 15 g $TKN \cdot m^{-3} \cdot d^{-1}$), $HRAP_1$ was more efficient than $HRAP_2$. LEDs in $HRAP_2$ used 1.4 times (S-0 to S-II), 2.3 times (S-III and S-IV) and 3.4 (S-V) times the total energy consumed to operate the conventional HRAP. The ratio of energy consumed by the LEDs per kg of pollutant removed in $HRAP_2$ over the total energy consumed per kg of pollutant removed in $HRAP_2$ varied from 0.6 (for COD, S-0 and S-I) to 6 (for TAN, S-V) (Fig. 5a, 5e, 5i, 5m). Even under the highest wattage, $HRAP_2$ presented similar or lower electricity consumption than other digestate treatment technologies such as membrane filtration, drying, composting or NH_3 stripping (Vázquez-Rowe *et al*., 2014). Removal efficiencies up to 80% at high COD influent volumetric loads of up to 300 $g \cdot m^{-3} \cdot d^{-1}$ have been reported in the literature during the treatment of urban wastewater and digestates (Torres-Franco *et al*., 2020). The results from S-II to S-IV suggested that at least 0.15 to 0.26 $\mu mol \cdot s^{-1} \cdot mgTSS^{-1}$ of red LED light should be supplied per cubic meter of reactor to sustain the photosynthetic growth of microalgae below the photic zone. The economic feasibility of LED-enhanced HRAPs should be carefully assessed in order to determine whether the extra capital and energy costs derived from LED power supply can be compensated by savings in land costs. Pretreatments for increasing TSS removal in the influent can contribute to reducing LED power requirement and energy consumption.

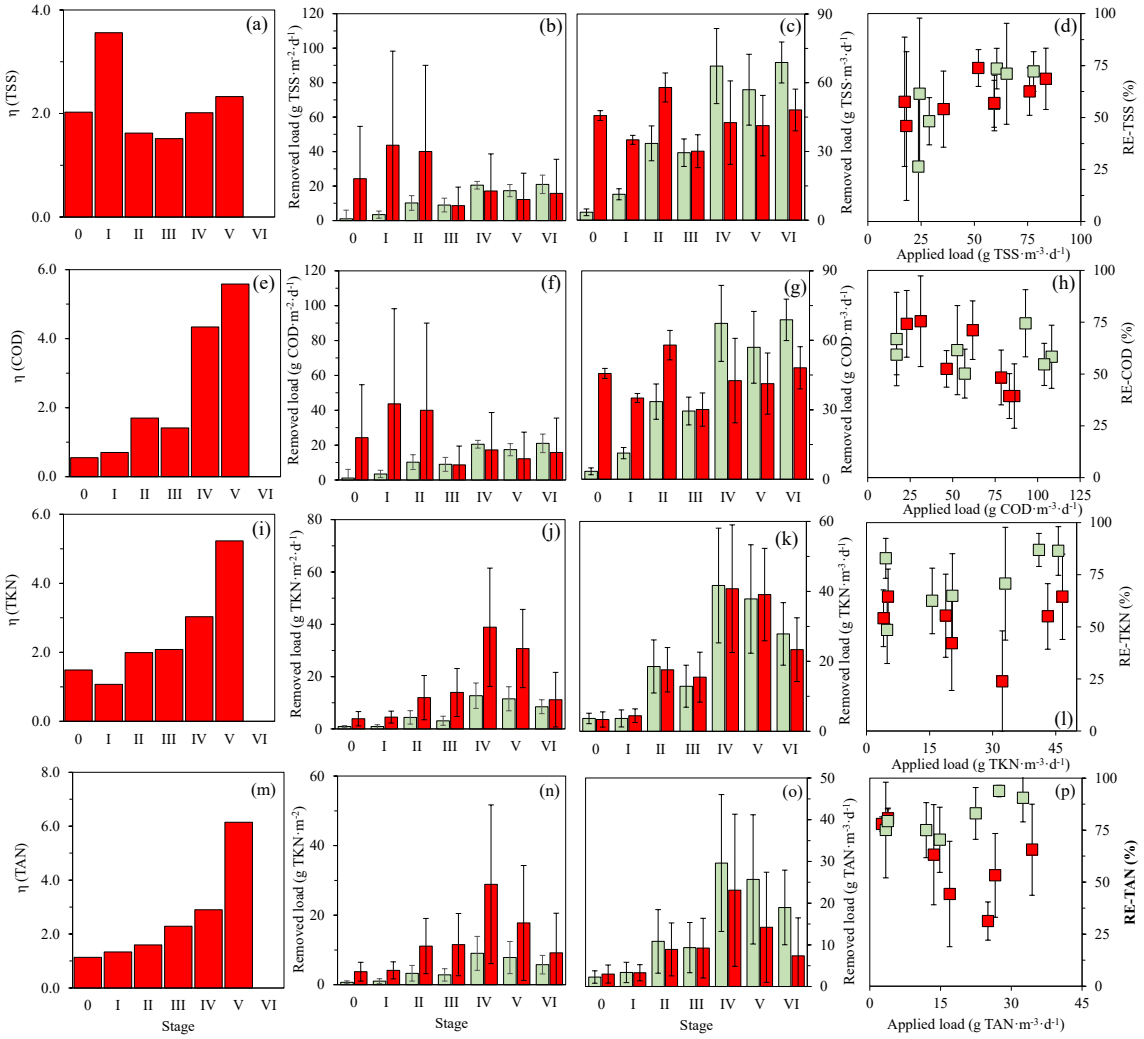

Figure 5. The η factor is defined as LED-related energy consumption per kg of pollutant removed in $HRAP_2$ divided by the total energy consumption per kg of pollutant removed in $HRAP_1$ for (a) TSS, (e) COD, (i) TKN and (m) TAN; Removal rates of TSS, COD, TKN and TAN per unit of HRAP's area (b, f, j, n) and volume (c, g, k, o); and removal efficiencies (RE) as a function of applied load (g $m^{-3}\cdot d^{-1}$) of TSS (d), COD (h), TAN (l) and TKN (p) in the $HRAP_1$ (■) and $HRAP_2$ (■).

Finally, despite the low microalgae productivities recorded under operation at long SRT, both HRAPs showed potential for recovering N and P for agricultural purposes, as evidenced by the average recovery factors in the wasted biomass ranging 8-17% and 6-34% for TN and of 10-45% and 5-48% for TP in $HRAP_1$ and $HRAP_2$, respectively. Additionally, the N available in the effluent was mainly present in the form of Org-N and N_{NO} (TAN

589 accounted for 24±9% of TN in the effluent of $HRAP_1$ and 43±17% in $HRAP_2$), conversely
590 to the average TAN 69±6% of TN in the influent digestate). This nitrogen shares in the
591 HRAPs significantly decreased the risk of NH_3 emissions when applying the effluent
592 instead of the raw digestate to agricultural soil as a fertilizer (Tiwari *et al*., 2015). Nitrogen
593 balances showed that operation at 25% and 50%-digestate decreased the FAN to less than
594 10% in the HRAPs; thus, avoiding high NH_3 emissions during digestate treatment.
595 Operation under shorter SRTs may increase microalgal productivities and nutrients
596 recovery in both ponds.

597 4 **Conclusions**

598 The long-term operation of a conventional HRAP and a deep LED-enhanced HRAP
599 treating increasing dilutions of food waste digestate ((5%, 25%, and 50% (v/v)) showed the
600 potential of conventional HRAPs to treat food waste digestate and to produce value-added
601 microalgae biomass, and the feasibility of a deep, LED-enhanced HRAP to match the
602 performance of the conventional HRAP. The maximum COD, TAN, TKN and TP removal
603 efficiencies achieved by the conventional HRAP were 74±16%, 87±8%, 94±3% and
604 59±12%, respectively. The bioremediation performance of the conventional HRAP was
605 limited mainly by the long SRT and CO_2 limitations. On the other hand, the deep LED-
606 enhanced HRAP showed a similar performance to that of the conventional HRAP for
607 digestate dilutions of 5% to 25%, but microalgae growth was seriously inhibited at
608 digestate dilutions of 50%. The deep LED-enhanced HRAP was efficient treating up to 75
609 g $COD \cdot m^{-3} \cdot d^{-1}$, 20 g $TAN \cdot m^{-3} \cdot d^{-1}$, 15 g $TKN \cdot m^{-3} \cdot d^{-1}$, and reduced the areal footprint of
610 conventional HRAPs by 75%. Despite these limitations of the LED-enhanced HRAP, the
611 control of influent solids and the increase of LED power, when economically feasible, may

612 increase its efficiency in the treatment of high-strength digestates, allowing the use of
613 microalgae-based treatments in cases where land costs render the use of conventional
614 HRAPs prohibitive. Nitrogen and phosphorus recoveries in the biomass accounted for 8-
615 17% and 6-34% for TN and of 10-45% and 5-48% for TP for $HRAP_1$ and $HRAP_2$,
616 respectively, showing potential for agricultural application of the biomass. The economic
617 feasibility of LED-enhanced HRAP should be carefully assessed in order to determine
618 whether the extra capital and energy costs derived from LED power supply can be
619 compensated by savings in land costs.

620 5 **Acknowledgments**

621 The authors acknowledge the Laboratory of Biomarkers in Clinical and Toxicological
622 Analysis of the School of Pharmacy at UFMG and the support of Gabriel Freitas with the
623 implantation of the systems. The authors also acknowledge the funding support of
624 FAPEMIG, through project 694 - FAPEMIG – APQ-02752-14, the CNPq for the scholarship
625 141428/2016-3, the National Inst. of Sci.&Tech. on Sustainable Sewage Treatment Plants
626 (INCT Sustainable Sewage Treatment Plants) and the Royal society (ICA\R1\191241). The
627 financial support from the Regional Government of Castilla y León is also gratefully
628 acknowledged (CLU 2017-09).

629 6 **References**

630 [1] Alcántara, C.; Muñoz, R.; Norvill, Z.; Plouviez, M.; Guieysse, B. Nitrous oxide
631 emissions from high rate algal ponds treating domestic wastewater. Bioresour Technol, v.
632 177, p. 110-117, 2015.https://doi.org/10.1016/j.biortech.2014.10.134

[2] Anbalagan, A., Schwede, S., Lindberg, C. E Nehrenheim, E. Influence of hydraulic retention time on indigenous microalgae and activated sludge process. Water Res, v. 91, p. 277-284, 2016.https://doi.org/10.1016/j.watres.2016.01.027

[3] Arcila, J. S.; Buitrón, G. Microalgae–bacteria aggregates: effect of the hydraulic retention time on the municipal wastewater treatment, biomass settleability and methane potential. J Chem Technol Biotechnol, v. 91, n. 11, p. 2862-2870, 2016.https://doi.org/10.1002/jctb.4901

[4] Ayre, J.; Moheimani, N.; Borowitzka, M. Growth of microalgae on undiluted anaerobic digestate of piggery effluent with high ammonium concentrations. Algal Res, v. 24, p. 218-226, 2017.https://doi.org/10.1016/j.algal.2017.03.023

[5] Bai, X.; Gu, H.; Li, Y. Coimmobilized microalgae and nitrifying bacteria for ammonium removal. IJESD, v. 7, n. 6, p. 406, 2016. 10.7763/IJESD.2016.V7.809

[6] Benemann, J. R. Bio-fixation of CO_2 and greenhouse gas abatement with microalgae-technology roadmap. Final Report to the US Department of Energy. National Energy Technology Laboratory, 2003.

[7] Blanken, W.; Cuaresma, M.; Wijffels, R. H.; Janssen, M. Cultivation of microalgae on artificial light comes at a cost. Algal Res, v. 2, n. 4, p. 333-340, 2013.https://doi.org/10.1016/j.algal.2013.09.004

[8] Buchanan, N. A.; Young, P.; Cromar, N. J.; Fallowfield, H. J. Performance of a high rate algal pond treating septic tank effluent from a community wastewater management scheme in rural South Australia. Algal Res, v. 35, p. 325-332, 2018.https://doi.org/10.1016/j.algal.2018.08.036

[9] Cagnetta, C.; Saerens, B.; MEerburg, F. A.; Decru, S. O.; Broeders, E.; Menkveld, W.; Vandekerckhove, T. G.; De Vrieze, J.; Vlaeminck, S. E.; Verliefde, A. R.; De Gusseme, B.; Weemaes, M.; Rabaey, K. High-rate activated sludge systems combined with dissolved air flotation enable effective organics removal and recovery. Bioresour Technol, v. 291, p. 121833, 2019.https://doi.org/10.1016/j.biortech.2019.121833

[10] Collos, Y., Harrison, P.J. Acclimation and toxicity of high ammonium concentrations to unicellular algae, Mar. Pollut. Bull. 80, 8–23, 2014.https://doi.org/10.1016/j.marpolbul.2014.01.006.

[11] Chuka-Ogwude, D.; Ogbonna, J.; Moheimani, N. R. A review on microalgal culture to treat anaerobic digestate food waste effluent. Algal Res, v. 47, p. 101841, 2020.https://doi.org/10.1016/j.algal.2020.101841

[12] Cohen, J., & Cohen, P. (1983). Applied multiple regression correlation analysis for the behavioral sciences (Second edition). New York: Erlbaum.

[13] Danyali, S.; Moteiri, L. PV Powered LED Street Lights Optimization Using Zeta-Sepic converter and Photo-Electro-Thermal Theory. International Journal of Industrial Electronics, Control and Optimization, 2020. 10.22111/IECO.2020.32127.1222

[14] De Godos, I.; Blanco, S.; García-Encina, P. A.; Becares, E.; Muñoz, R. Long-term operation of high rate algal ponds for the bioremediation of piggery wastewaters at high loading rates. Bioresour Technol, v. 100, n. 19, p. 4332-4339, 2009.https://doi.org/10.1016/j.biortech.2009.04.016

[15] De Godos, I.; Arbib, Z.; Lara, E.; Rogalla, F. Evaluation of High Rate Algae Ponds for treatment of anaerobically digested wastewater: Effect of CO_2 addition and

677 modification of dilution rate. Bioresour Technol, v. 220, p. 253-261,
678 2016.https://doi.org/10.1016/j.biortech.2016.08.056

679 [16] Eland, L. E.; Davenport, R. J.; Santos, A. B. D.; Mota Filho, C. R. Molecular
680 evaluation of microalgal communities in full-scale waste stabilisation ponds. Environ
681 Technol, v. 40, n. 15, p. 1969-1976, 2019.https://doi.org/10.1080/09593330.2018.1435730

682 [17] García, J.; Green, B. F.; Lundquist, T.; Mujeriego, R.; Hernández-Mariné, M.;
683 Oswald, W. J. Long term diurnal variations in contaminant removal in high rate ponds
684 treating urban wastewater. Bioresour Technol, v. 97, n. 14, p. 1709-1715,
685 2006.https://doi.org/10.1016/j.biortech.2005.07.019

686 [18] Garfí, M.; Flores, L.; Ferrer, I. Life cycle assessment of wastewater treatment
687 systems for small communities: activated sludge, constructed wetlands and high rate algal
688 ponds. J Clean Prod, v. 161, p. 211-219, 2017.https://doi.org/10.1016/j.jclepro.2017.05.116

689 [19] Gerardi, M. H. The microbiology of anaerobic digesters, pp 32. John Wiley & Sons,
690 2003. DOI:10.1002/0471468967

691 [20] Goldman, J. C.; Dennett, M. R.; Riley, C. B. Effect of nitrogen-mediated changes in
692 alkalinity on pH control and CO_2 supply in intensive microalgal cultures. Biotechnol
693 Bioeng, v. 24, n. 3, p. 619-631, 1982.https://doi.org/10.1002/bit.260240308

694 [21] Hom-Diaz, A., Norvill, Z. N., Blánquez, P., Vicent, T., & Guieysse, B.
695 Ciprofloxacin removal during secondary domestic wastewater treatment in high rate algal
696 ponds. *Chemosphere*, *180*, 33-41, 2017.https://doi.org/10.1016/j.chemosphere.2017.03.125

697 [22] How, S. W., Chua, A. S. M., Ngoh, G. C., Nittami, T., & Curtis, T. P. Enhanced
698 nitrogen removal in an anoxic-oxic-anoxic process treating low COD/N tropical

699 wastewater: Low-dissolved oxygen nitrification and utilization of slowly-biodegradable
700 COD for denitrification. Sci. Total Environ., *693*, 133526, 2019

701 [23] Jankowska, E.; Zieliński, M.; Dębowski, M.; Oleśkowicz-Popiel, P. Anaerobic
702 digestion of microalgae for biomethane production. In: Second and Third Generation of
703 Feedstocks (pp. 405-436). Elsevier, 2019.https://doi.org/10.1016/B978-0-12-815162-
704 4.00015-X

705 [24] Jia, H.; Yuan, Q. Removal of nitrogen from wastewater using microalgae and
706 microalgae–bacteria consortia. Cogent Environmental Science, v.2, n. 1, p. 1275089,
707 2016.https://doi.org/10.1080/23311843.2016.1275089

708 [25] Jeon, Y. C.; Cho, C. W.; Yun, Y. S. Measurement of microalgal photosynthetic
709 activity depending on light intensity and quality. Biochem Eng J, v. 27, n. 2, p. 127-131,
710 2005 https://doi.org/10.1016/j.bej.2005.08.017

711 [26] Kim, B.; Kim, D.; Choi, J.; Kang, Z.; Cho, D.; Kim, J.; Oh, H.; Kim, H.
712 Polypropylene Bundle Attached Multilayered Stigeoclonium Biofilms Cultivated in
713 Untreated Sewage Generate High Biomass and Lipid Productivity J Microbiol Biotechn, v.
714 25, n. 9, p. 1547-1554, 2015.

715 [27] Kim, B. H.; Choi, J. E.; Cho, K.; Kang, Z.; Ramanan, R.; Moon, D. G.; Kim, H. S.
716 Influence of water depth on microalgal production, biomass harvest, and energy
717 consumption in high rate algal pond using municipal wastewater. J Microbiol Biotechn, v.
718 28, n. 4, p. 630-637, 2018.https://doi.org/10.4014/jmb.1801.01014

719 [28] Mahapatra, D. M.; Chanakya, B. N.; Ramachandra, T. V. *Euglena* sp. as a suitable
720 source of lipids for potential use as biofuel and sustainable wastewater treatment. J Appl
721 Phycol, v. 25, n. 3, p. 855-865, 2013.https://doi.org/10.1007/s10811-013-9979-5

722 [29] Marin, D.; Posadas, E.; Cano, P.; Pérez, V.; Blanco, S.; Lebrero, R.; Muñoz, R.
723 Seasonal variation of biogas upgrading coupled with digestate treatment in an outdoors
724 pilot scale algal-bacterial photobioreactor. Bioresour Technol, v. 263, p. 58-66,
725 2018.https://doi.org/10.1016/j.biortech.2018.04.117

726 [30] Nakamura, H., Shiozaki, T., Gonda, N., Furuya, K., Matsunaga, S., & Okada, S.
727 Utilization of ammonium by the hydrocarbon-producing microalga, Botryococcus braunii
728 Showa. Algal Res, v *25*, 445-451, 2017. https://doi.org/10.1016/j.algal.2017.06.007

729 [31] Nwoba, E. G.; Ayre, J. M.; Moheimani, N. R.; Ubi, B. E.; Ogbonna, J. C. Growth
730 comparison of microalgae in tubular photobioreactor and open pond for treating anaerobic
731 digestion piggery effluent. Algal Res, v. 17, p. 268-276,
732 2016.https://doi.org/10.1016/j.algal.2016.05.022

733 [32] Ogbonna, I. O.; Ogbonna, J. C. Effects of carbon source on growth characteristics
734 and lipid accumulation by microalga *Dictyosphaerium* sp. with potential for biodiesel
735 production. *Energy and Power Engineering*, v. 10, n. 2, p. 29-42, 2018.

736 [33] Plouviez, M.; Chambonnière, P.; Shilton, A.; Packer, M. A.; Guieysse, B. Nitrous
737 oxide (N_2O) emissions during real domestic wastewater treatment in an outdoor pilot-scale
738 high rate algae pond. Algal Res, v. 44, p. 101670, 2019.
739 https://doi.org/10.1016/j.algal.2019.101670

740 [34] Posadas, E.; Del Mar Morales, M.; Gomez, C.; Acién, F. G.; Muñoz, R. Influence of
741 pH and CO_2 source on the performance of microalgae-based secondary domestic
742 wastewater treatment in outdoors pilot raceways. Chem Eng J , v. 265, p. 239-248,
743 2015.https://doi.org/10.1016/j.cej.2014.12.059

744 [35] Qilu, C.; Ligen, X.; Fangmin, C.; Gang, P.; Qifa, Z. Bicarbonate-rich wastewater as
745 a carbon fertilizer for culture of Dictyosphaerium sp. of a giant pyrenoid. *Journal of Cleaner*
746 *Production*, v. 202, p. 439-443, 2018.

747 [36] Rada-Ariza, A. M.; Fredy, D.; Lopez-Vazquez, C. M.; Van Der Steen, N. P.; Lens,
748 P. Ammonium removal mechanisms in a microalgal-bacterial sequencing-batch
749 photobioreactor at different solids retention times. Algal Res, v. 39, p. 101468,
750 2019.https://doi.org/10.1016/j.algal.2019.101468

751 [37] Rice, E. W.; Baird, R. B.; Eaton, A. D.; Clesceri, L. S. Standard methods for the
752 examination of water and wastewater. American Public Health Association, American
753 Water Works Association, and Water Environment Federation, 2012.

754 [38] Singh, S. P.; Singh, P. Effect of temperature and light on the growth of algae
755 species: a review. Renew Sust Energ Rev, v. 50, p. 431-444,
756 2015.https://doi.org/10.1016/j.rser.2015.05.024

757 [39] Sutherland, D. L.; Turnbull, M. H.; Craggs, R. J. Increased pond depth improves
758 algal productivity and nutrient removal in wastewater treatment high rate algal
759 ponds. Water Res, v. 53, p. 271-281, 2014.https://doi.org/10.1016/j.watres.2014.01.025

760 [40] Tampio, E.; Ervasti, S.; Rintala, J. Characteristics and agronomic usability of
761 digestates from laboratory digesters treating food waste and autoclaved food waste. J Clean
762 Prod, v. 94, p. 86-92, 2015.https://doi.org/10.1016/j.jclepro.2015.01.086

763 [41] Tiwary, A., Williams, I. D., Pant, D. C., & Kishore, V. V. N. Assessment and
764 mitigation of the environmental burdens to air from land applied food-based
765 digestate. *Environmental Pollution*, *203*, 262-270, 2015.

766 [42] Torres-Franco, A. F.; Araujo, S.; Passos, F.; De Lemos Chernicharo, C. A.; Mota
767 Filho, C. R.; Cunha Figueredo, C. Treatment of food waste digestate using microalgae-
768 based systems with low-intensity light-emitting diodes. Water Sci & Tech, v. 78, n. 1, p.
769 225-234, 2018.https://doi.org/10.2166/wst.2018.198

770 [43] Torres-Franco, A., Passos, F., Figueredo, C. Muñoz R. Current advances in
771 microalgae-based treatment of high-strength wastewaters: challenges and opportunities to
772 enhance wastewater treatment performance. Rev Environ Sci Biotechnol,
773 2020.https://doi.org/10.1007/s11157-020-09556-8

774 [44] Uggetti, E.; García, J.; Álvarez, J. A.; García-Galán, M. J. Start-up of a microalgae-
775 based treatment system within the biorefinery concept: from wastewater to bioproducts.
776 Water Sci & Tech, v. 78, n. 1, p. 114-124, 2018. https://doi.org/10.2166/wst.2018.195

777 [45] Yan, C.; Muñoz, R.; Zhu, L.; Wang, Y. The effects of various LED (light emitting
778 diode) lighting strategies on simultaneous biogas upgrading and biogas slurry nutrient
779 reduction by using of microalgae *Chlorella* sp. *Energy*, v. 106, p. 554-561,
780 2016.https://doi.org/10.1016/j.energy.2016.03.033

781 [46] Yamane, Y. I.; Utsunomiya, T.; Watanabe, M.; Sasaki, K. Biomass production in
782 mixotrophic culture of *Euglena gracilis* under acidic condition and its growth
783 energetics. Biotechnol. Lett, v. 23, n. 15, p. 1223-1228,
784 2001.https://doi.org/10.1023/A:1010573218863

785 [47] Vaneeckhaute, C.; Lebuf, V.; Michels, E.; Belia, E.; Vanrolleghem, P. A.; Tack, F.
786 M.; Meers, E. Nutrient recovery from digestate: systematic technology review and product
787 classification. Waste Biomass Valorization, v. 8, n. 1, p. 21-40,
788 2017.https://doi.org/10.1007/s12649-016-9642-x

789 [48] Van Den Hende, S.; Vervaeren, H.; Saveyn, H.; Maes, G.; Boon, N. Microalgal
790 bacterial floc properties are improved by a balanced inorganic/organic carbon ratio.
791 Biotechnol Bioeng , v. 108, n. 3, p. 549-558, 2011.https://doi.org/10.1002/bit.22985

792 [49] Vázquez-Rowe, I., Golkowska, K., Lebuf, V., Vaneeckhaute, C., Michels, E.,
793 Meers, E., ... & Koster, D. (2015). Environmental assessment of digestate treatment
794 technologies using LCA methodology. *Waste management*, *43*, 442-459.

795 [50] Vassalle, L.; Díez-montero, R.; Machado, A. T. R.; Moreira, C.; Ferrer, I.; Mota, C.
796 R.; Passos, F. Upflow anaerobic sludge blanket in microalgae-based sewage treatment: co-
797 digestion for improving biogas production. Bioresour Technol, v. 300, p. 122677,
798 2020a.https://doi.org/10.1016/j.biortech.2019.122677

799 [51] Vassalle L, García-Galán MJ, Aquino SF, et al. Can high rate algal ponds be used as
800 post-treatment of UASB reactors to remove micropollutants? Chemosphere 248, 125969,
801 2020b.https://doi.org/10.1016/j.chemosphere.2020.125969

802 [52] Webb, J. P.; Van Keulen, M.; Wong, S. K. S.; Hamley, E.; Nwoba, E.; Moheimani, N.
803 R. Light spectral effect on a consortium of filamentous green algae grown on anaerobic
804 digestate piggery effluent (ADPE). *Algal Res*, v. 46, p. 101723, 2019.

805

ASSESSMENT OF A DEEP, LED-ENHANCED HIGH RATE ALGAL POND FOR THE TREATMENT OF DIGESTATE

Torres-Franco, A.F.[1], Figueredo, C. C.[2], Barros L.[1], Gücker B.[3], Boechät, I.G.[3], Muñoz R.[4,5], Mota C.R.[1*]

[1]*Department of Sanitary and Environmental Engineering, Federal University of Minas Gerais- Belo Horizonte 31270-010, Brazil;*
[2]*Institute of Biological Sciences, Federal University of Minas Gerais Belo Horizonte 31270-010, Brazil;*
[3] *Department of Geosciences, Federal University of São João del-Rei, Praça Dom Helvécio 74, São João del-Rei, MG 36301-160, Brazil;*
[4]*Department of Chemical Engineering and Environmental Technology, School of Industrial Engineering, Valladolid University, Dr. Mergelina s/n., Valladolid 47011, Spain;*
[5]*Institute of Sustainable Processes, Valladolid University, Dr. Mergelina s/n., Valladolid 47011, Spain.*

*-*Corresponding author:* cesar@desa.ufmg.br*

Supplementary Material

S.1 Mass balances

Mass balances of TSS, COD, nitrogen compounds and TP in $HRAP_1$ and $HRAP_2$ were calculated using the measured concentrations and estimated flow rates. Removal efficiencies were estimated based on digestate flow rates and concentrations of the influent digestate and effluents from the secondary settlers. The removal efficiencies (RE) of the target parameters *(i)* were calculated for each HRAP (*h*) and operational condition (*j*) according to Eq. S.1:

$$RE_{i,h,j}(\%) = \frac{(C_{i,h,j}\cdot Q_f)-(C_{i,h,j(e)}\cdot Qe_{i,h,j})}{(C_{i,h,j(in)}\cdot Q_f)}\cdot 100$$

(Eq. S.1)

Where C_i is the concentration of the target parameter in the influent *(in)* and effluent *(e)* of each HRAP. Q_f corresponds with the flow rate of each feeding (125 L·d^{-1}) and Q_e corresponds to the effluent flow rate of each HRAP (h) and stage (j), defined by Eq. S.2, which accounts for the flow rates of rainfall $\left(P_{h,j}\right)$ and evaporation from each HRAP $\left(Q_{ev_{h,j}}\right)$.

$$Q_{e_{h,j}} = Q_f + P_{h,j} - Q_{ev_{h,j}}$$

(Eq. S.2)

The rainfall flowrate was calculated as the sum of the hourly rainfall per day (L·d^{-1}) whereas Q_{ev} was defined as $Q_{ev_{h,j}} = Ev_{h,j} \cdot A_{HRAP}$, where $Ev_{h,j}$ corresponded to the areal evaporation rate of HRAP$_1$ and HRAP$_2$ during each stage and A_{HRAP} to the surface area of each pond. $Ev_{h,j}$ was estimated as the daily mean of volume losses in each pond per unit of area. To calculate the N mass balance, it was assumed that the N entering the ponds (N_{in}) left the HRAP in four different forms: 1) assimilated into biomass (OrgN); 2) converted into NO_2^- or NO_3^- (N_{NO}); 3) as dissolved TAN, and 4) volatilized as NH_3 or N_2 (N_{lost}). Each term of the balance was calculated according to Eq S.3-S.4:

$$M_{N_{in}{}_{h,j}} = Q_f(TKN_{(in)_{h,j}} + N_{NO(in)_{h,j}})$$

(Eq. S.3)

$$N_{LOST}{}_{h,j} = \left(M_{N_{in}{}_{h,j}} - Q_{e_{h,j}}(\mathrm{TKN}_e + N_{NO_e})_{h,j} - Q_{WB_{h,j}}(\mathrm{TKN}_H + N_{NO_H})_{h,j}\right) / M_{N_{in}{}_{h,j}}$$

(Eq.S.4)

Where Q_{WB} corresponds to the flow rate of biomass wasted from the HRAP (WB) and $TKN_{(H)} + N_{NO(H)}$ to the concentrations of TKN and N_{NO} measured in the HRAP (H). The mass of N assimilated was also estimated for each HRAP during each stage as (Eq. S.5):

$$\%N\ assimilated_{h,j} = \frac{(M_{Org-N})_{e_{h,j}} + (M_{Org-N})_{WB_{h,j}} - (M_{Org-N})_{In_{h,j}}}{M_{N_{in}}}\ x\ 100\%$$

(Eq. S.5)

Where $(M_{Org-N})_{h,j}$ is the mass flow rate of organic nitrogen in the effluent (*e*), waste biomass (*WB*), and influent (*in*) of each HRAPs (*h*) for the operational stage *j*. The biomass productivity of each pond was estimated according to Eq. S.6 (Park *et al*., 2012) and the TN and TP recoveries in the waste biomass were estimated according to Eq. S7 and S.8

$$Productivity_{h,j} = \frac{VSS_{(H)_{h,j}} Q_{(H)_{h,j}} - VSS_{(R)_{h,j}} Q_{(R)_{h,j}}}{A_{HRAP_i}}\ x\ 100\%$$

(Eq. S.6)

$$\%N\ recovery_{h,j} = \frac{Q_{WB_{h,j}} (\mathrm{TKN_{(H)}}_{h,j} + \mathrm{N_{NO}}_{(H)_{h,j}})}{M_{N_{(in)_{h,j}}}}\ x\ 100\%$$

(Eq. S.7)

$$\%P\ recovery_{h,j} = \frac{Q_{WB_{h,j}} (\mathrm{TP_{(H)}}_{h,j})}{M_{P_{(in)_{h,j}}}}\ x\ 100\%$$

(Eq. S.8)

Where $VSS_{(H)}$ and $VSS_{(R)}$ are the VSS concentrations in each HRAP and each recirculation line, $Q_{(H)} = Q_e - Q_R$ and Q_R is the flow rate of biomass recirculation (75 $L \cdot d^{-1}$). $M_{N_{in}}$ and $M_{P_{in}}$ stand for the mass of TN and TP in the raw digestate (*in*), estimated as Eq. S.3 and

874 $M_{P_{in}{}_{h,j}}$= Q_f $(\mathrm{TP}_{(\mathrm{in})}{}_{h,j})$. Finally, based in the mass of pollutants removed in each systems,

875 removal rates and energy consumptions factors were estimated following equations S.9-S.13

876 $$kWh \cdot (0.125\ m^3 \cdot d^{-1})^{-1}{}_{HRAP_{h,j}} = \frac{kWh \cdot d^1{}_{h,j}}{0.125\ m^3 \cdot d^{-1}}\ x\ 100\%$$

877 (Eq. S.9)

878 $$kWh \cdot kg\ TSS^{-1}{}_{HRAP_{h,j}} = \frac{kWh \cdot d^1{}_{h,j}}{kg\ TSS\ removed \cdot d^{-1}{}_{i,j}}\ x\ 100\%$$

879 (Eq. S.10)

880 $$kWh \cdot kg\ COD^{-1}{}_{HRAP_{h,j}} = \frac{kWh \cdot d^1{}_{h,j}}{kg\ COD\ removed \cdot d^{-1}{}_{h,j}}\ x\ 100\%$$

881 (Eq. S.11)

882 $$kWh \cdot kg\ TKN^{-1}{}_{HRAP_{h,j}} = \frac{kWh \cdot d^1{}_{h,j}}{kg\ TKN\ removed \cdot d^{-1}{}_{h,j}}\ x\ 100\%$$

883 (Eq. S.12)

884 $$kWh \cdot kg\ TAN^{-1}{}_{HRAP_{h,j}} = \frac{kWh \cdot d^1{}_{h,j}}{kg\ TKN\ removed \cdot d^{-1}{}_{h,j}}\ x\ 100\%$$

885 (Eq. S.13)

886 $$\eta_i = \frac{\frac{kWh/d_{h2}\ (total) - kWh/d_{h2}\ (paddlewheel+pump}{kg\ pollutant\ removed \cdot d^{-1}{}_{h2,j}})}{\frac{kWh \cdot d^1{}_{h1,j}}{kg\ pollutnat\ removed \cdot d^{-1}{}_{h1j}}}\ x\ 100\%$$

887 (Eq. S.14)

888

889

S.2 COD, TKN, TAN, NNO, VSS and TSS concentrations in the influent digestate (in), HRAP (H), recirculation (R) and effluents (Ef) in the conventional HRAP ($HRAP_1$, H_1) and the LED-enhanced HRAP ($HRAP_2$, H_2)

Table S.1 – COD and sCOD concentrations in the influent digestate (in), HRAP (H), recirculation (R) and effluents (Ef) in the conventional HRAP ($HRAP_1$, H_1) and the LED-enhanced HRAP ($HRAP_2$, H_2) (Mean ± S.D (Data number))

Parameter		Stage						
		0	I	II	III	IV	V	VI
$COD_{(in)}$	H_1	212 ± 166 (12)	185± 94 (8)	528± 88 (7)	571± 184 (10)	1066 ± 90 (12)	1038 ± 67 (9)	928 ±134 (6)
	H_2	231 ± 140 (12)	183± 92 (8)	490 ± 108 (7)	609 ± 188 (10)	1074 ± 103 (12)	1058 ± 93 (9)	924 ±162 (6)
$sCOD_{(in)}$	H_1	51 ± 29 (4)	10 ± 5 (7)	138 ± 40 (7)	185 ± 22 (10)	339 ± 167 (12)	304 ± 106 (9)	421 ± 327 (6)
	H_2	52 ± 31 (4)	17 ± 14 (7)	133 ± 58 (7)	140 ± 135 (10)	308 ± 141 (12)	440 ± 307 (9)	447 ± 188 (6)
$sCOD_{(H)}$	H_1	83 ± 49 (7)	57 ± 43 (8)	148 ± 76 (7)	443 ± 233 (10)	637 ± 192 (12)	663 ± 341 (9)	559 ± 378 (6)
	H_2	80 ± 26 (6)	24 ± 20 (8)	155 ± 85 (7)	417 ± 203 (10)	559 ± 204 (12)	473 ± 247 (9)	667 ± 363 (6)
$sCOD_{(R)}$	H_1	-	69 ± 72 (8)	182 ± 128 (7)	755 ± 579 (10)	1065 ± 515 (12)	895 ± 453 (9)	2598 ± 2240 (6)
	H_2	-	44 ± 58 (8)	122 ± 107 (7)	563 ± 180 (10)	1468 ± 1270 (12)	885 ± 457 (9)	2179 ± 1926 (6)
$COD_{(Ef)}$	H_1	51 ± 28 (10)	93 ± 51 (8)	223 ± 103 (7)	338 ± 73 (10)	485 ± 117 (12)	542 ± 107 (9)	279 ± 119 (6)
	H_2	58 ± 35 (10)	40 ± 17 (8)	186 ± 75 (7)	284 ± 98 (10)	663 ± 186 (12)	690 ± 102 (9)	606 ± 70 (6)
$sCOD_{(Ef)}$	H_1	49 ± 13 (7)	48 ± 26 (8)	54 ± 32 (7)	177 ± 124 (10)	240 ± 82 (12)	151 ± 26 (9)	123 ± 79 (6)
	H_2	47 ± 30 (7)	19 ± 14 (8)	74 ± 28 (7)	127± 56 (10)	235 ± 77 (12)	272 ± 54 (9)	282 ±82 (6)

Table S.2 – TAN concentrations in the influent digestate (in), HRAP (H), recirculation (R) and effluents (Ef) in the conventional HRAP ($HRAP_1$, H_1) and the LED-enhanced HRAP ($HRAP_2$, H_2) (Mean ± S.D (Data number))

Parameter		Stage						
		0	I	II	III	IV	V	VI
$TAN_{(in)}$	H_1	34 ± 19 (7)	38 ± 21(8)	148± 36 (7)	120 ± 43(10)	328 ± 135 (12)	274 ± 31(9)	224 ± 37 (6)
	H_2	34 ± 23 (7)	39 ± 17(8)	144 ± 34(7)	136 ± 47(10)	342 ± 121 (12)	266 ± 45(9)	250 ± 58 (6)
$TAN_{(H)}$	H_1	1 ± 2 (7)	5 ± 2 (8)	50 ± 25 (7)	43 ± 14 (10)	61 ± 31 (12)	52 ± 39 (9)	33 ± 20 (6)
	H_2	3 ± 3 (7)	9 ± 4 (8)	100 ± 33(7)	43 ± 18 (10)	132 ± 75 (12)	176 ± 60(9)	204 ± 108 (6)
$TAN_{(R)}$	H_1	-	10 ± 4 (8)	44 ± 27 (7)	51 ± 12 (10)	38 ± 16 (12)	22 ± 8 (9)	39 ± 25 (6)
	H_2	-	8 ± 2 (8)	77 ± 45 (7)	35 ± 15 (10)	134 ± 58 (12)	184 ± 27(9)	236 ± 50 (6)
$TAN_{(Ef)}$	H_1	7 ± 6 (7)	14 ± 20(8)	47 ± 23 (7)	34 ± 12 (10)	29 ± 11 (12)	20 ± 9 (9)	48 ± 28 (6)
	H_2	3 ± 2 (7)	8 ± 3 (8)	81 ± 29 (7)	43 ± 22 (10)	115 ± 70 (12)	134 ± 53(9)	217 ± 70 (6)

Table S.3 – TKN concentrations in influent digestate (in), HRAP (H), recirculation (R) and effluents (Ef) for the conventional HRAP ($HRAP_1$, H_1) and the LED-enhanced HRAP ($HRAP_2$, H_2) (Mean ± S.D (Data number))

Parameter		Stage						
		0	I	II	III	IV	V	VI
$TKN_{(in)}$	H_1	46 ± 16 (7)	49 ± 21 (8)	204 ± 68 (7)	156 ± 55 (10)	463 ± 204 (12)	410 ± 147(9)	353 ± 51 (6)
	H_2	40 ± 19 (7)	51 ± 19 (8)	203 ± 57 (7)	188 ± 69 (10)	462 ±188 (12)	431 ± 133 (9)	323 ± 55 (6)
$TKN_{(H)}$	H_1	14 ± 6 (7)	37 ± 12 (8)	76 ± 27 (7)	77 ± 20 (10)	142 ± 48 (12)	140 ± 54 (9)	129 ± 95 (6)
	H_2	18 ± 20 (7)	28 ± 11 (8)	138 ± 22 (7)	83 ± 40 (10)	207 ± 91 (12)	309 ± 38 (9)	387 ± 82 (6)
$TKN_{(R)}$	H_1	-	43 ± 25 (8)	164 ± 62 (7)	234 ± 150 (10)	330 ± 224 (12)	487 ± 41 (9)	317 ± 177 (6)
	H_2	-	39 ± 29 (8)	209 ± 92 (7)	174 ± 75 (10)	494 ± 202 (12)	534 ± 105 (9)	202 ± 150 (6)
$TKN_{(Ef}$	H_1	11 ± 4 (7)	31 ± 19 (8)	68 ± 28 (7)	66 ± 21 (10)	59 ± 33 (12)	59 ± 35 (9)	120 ± 86 (6)
	H_2	8 ± 4 (7)	18 ± 8 (8)	112± 42 (7)	77 ± 32 (10)	157 ± 84 (12)	202 ± 59 (9)	297 ± 96 (6)

Table S.4 – nitrite-N + nitrate-N (N_{NO}) concentrations in influent digestate (in), HRAP (H), recirculation (R) and effluents (Ef) for the conventional HRAP ($HRAP_1$, H_1) and the LED-enhanced HRAP ($HRAP_2$, H_2) (Mean ± S.D(Data number))

Parameter		Stage						
		0	**I**	**II**	**III**	**IV**	**V**	**VI**
$N_{NO\ (in)}$	**H_1**	8 ± 8 (4)	7 ± 4 (8)	10 ± 8 (7)	3 ± 2 (10)	9 ± 5 (12)	16 ± 6 (9)	6 ± 1 (6)
	H_2	6 ± 9 (7)	10 ± 10 (8)	12 ± 12 (7)	3 ± 1 (10)	10 ± 6 (12)	14 ± 7 (9)	9 ± 6 (6)
$N_{NO\ (H)}$	**H_1**	3 ± 1 (7)	12 ± 7 (8)	38 ± 34 (7)	75 ± 30 (12)	127 ± 36 (12)	50 ± 48 (9)	58 ± 25 (6)
	H_2	6 ± 2 (7)	21 ± 10 (8)	37 ± 32 (7)	50 ± 36 (12)	7 ± 5 (12)	12 ± 8 (9)	5 ± 1 (6)
$N_{NO\ (R)}$	**H_1**	-	10 ± 9 (8)	19 ± 17 (7)	59 ± 37 (10)	21 ± 27 (12)	22 ± 21 (9)	6 ± 2 (6)
	H_2	-	12 ± 7 (8)	22 ± 17 (7)	27 ± 20 (10)	13 ± 16 (12)	11 ± 9 (9)	12 ± 5 (6)
$N_{NO\ (Ef)}$	**H_1**	2 ± 1 (8)	5 ± 3 (7)	36 ± 42 (7)	56 ± 43 (12)	46 ± 41 (12)	34 ± 12 (9)	24 ± 11 (6)
	H_2	6 ± 8 (8)	14 ± 8 (7)	59 ± 40 (7)	24 ± 31 (12)	13 ± 19 (12)	15 ± 7 (9)	8 ± 1 (6)

Table S.5 – TSS concentrations in influent digestate (in), HRAP (H), recirculation (R) and effluents (Ef) for the conventional HRAP ($HRAP_1$, H_1) and the LED-enhanced HRAP ($HRAP_2$, H_2) (Mean ± S.D (Data number))

Parameter		**Stage**						
		0	**I**	**II**	**III**	**IV**	**V**	**VI**
$TSS_{(in)}$	**H_1**	121 ± 96 (4)	95 ± 65 (8)	385 ± 109 (7)	288 ± 93 (10)	788 ± 234 (12)	593 ± 136 (9)	651 ± 92 (6)
	H_2	108 ± 98 (4)	68 ± 39 (8)	345 ± 129 (7)	355 ± 156 (10)	875 ± 309 (12)	769 ± 220 (9)	594 ± 52 (6)
$TSS_{(H)}$	**H_1**	132 ± 20 (9)	193 ± 57 (8)	310 ± 96 (7)	450 ± 74 (10)	831 ± 327 (12)	1606 ± 534 (9)	1406 ± 275 (6)
	H_2	64 ± 44 (9)	62 ± 12 (8)	280 ± 153 (7)	384 ± 167 (10)	801 ± 406 (12)	1141 ± 101 (9)	1245 ± 243 (6)
$TSS_{(R)}$	**H_1**	-	223 ± 180(8)	1215 ± 966 (7)	2403 ± 2215(10)	3804 ± 3462(12)	8789 ± 1862(9)	9563 ± 3950(6)
	H_2	-	311 ± 400(8)	1494 ± 1171(7)	2076 ± 1346(10)	4141 ± 2012(12)	6567 ± 2375(9)	4423 ± 235(6)
$TSS_{(Ef)}$	**H_1**	25 ± 25 (6)	75 ± 19 (8)	117± 25 (7)	143 ± 38 (10)	255 ± 126 (12)	304 ± 57 (9)	193 ± 104 (6)
	H_2	35 ± 28 (6)	36 ± 35 (8)	111 ± 25 (7)	144 ± 44 (10)	281 ± 147 (12)	312 ± 52 (9)	307 ± 59 (6)

Table S.6 – VSS concentrations in influent digestate (in), HRAP (H), recirculation (R) and effluents (Ef) for the conventional HRAP ($HRAP_1$, H_1) and the LED-enhanced HRAP ($HRAP_2$, H_2) (Mean ± S.D (Data number))

Parameter		**Stage**						
		0	**I**	**II**	**III**	**IV**	**V**	**VI**
$VSS_{(in)}$	**H_1**	98 ± 80 (4)	82 ± 61 (8)	371 ± 106 (7)	269 ± 81 (10)	701 ± 175 (9)	555 ± 112 (9)	577 ± 99 (6)
	H_2	92 ± 81 (4)	66 ± 37 (8)	329 ± 121 (7)	314 ± 120 (10)	785 ± 260 (9)	695 ± 191 (9)	533 ± 63 (6)
$VSS_{(H)}$	**H_1**	112 ± 98 (9)	163 ± 51 (8)	287 ± 63 (7)	424 ± 80 (10)	741 ± 276 (9)	1391 ± 434 (9)	1178 ± 267 (6)
	H_2	48 ± 41 (9)	60 ± 10 (8)	231 ± 82 (7)	353 ± 143 (10)	691 ± 330 (9)	994 ± 59 9()	1010 ± 208 (6)
VSS $_{(R)}$	**H_1**	-	186 ± 140(8)	1034 ± 817(7)	2021 ± 1842(10)	3273 ± 2922(9)	7660 ± 1655 (9)	8253 ± 3428(6)
	H_2	-	221 ± 281(8)	1207 ± 903(7)	1782 ± 1142(10)	3562 ± 1705(9)	5462 ± 2123 (9)	3673 ± 1999(6)
VSS $_{(Ef}$	**H_1**	21 ± 21 (6)	62 ± 14 (8)	104 ± 29 (7)	165 ± 36 (10)	241 ± 116 (9)	274 ± 60 (9)	154 ± 86 (6)
	H_2	24 ± 24 (6)	19 ± 10 (8)	96± 16 (7)	143 ± 38 (10)	253 ± 118 (9)	275 ± 45 (9)	270 ± 46 (6)

Table S.7 – TP concentrations in influent digestate (in), HRAP (H), recirculation (R) and effluents (Ef) for the conventional HRAP ($HRAP_1$, H_1) and the LED-enhanced HRAP ($HRAP_2$, H_2) (Mean ± S.D (Data number))

Parameter		Stage						
		0	**I**	**II**	**III**	**IV**	**V**	**VI**
$TP_{(in)}$	**H_1**	15 ± 10 (4)	7 ± 4 (8)	26 ± 9 (7)	11 ± 6 (10)	31 ± 9 (9)	28 ± 7 (9)	24 ± 8 (6)
	H_2	17 ± 7 (4)	8 ± 6 (8)	23 ± 7 (7)	12 ± 4 (10)	31 ± 8 (9)	26 ± 6 (9)	24 ± 5 (6)
$TP_{(H)}$	**H_1**	6 ± 2 (9)	7 ± 2 (8)	19 ± 4 (7)	15 ± 2 (10)	32 ± 11 (9)	29 ± 8 (9)	32 ± 8 (6)
	H_2	6 ± 1 (9)	6 ± 2 (8)	23 ± 5 (7)	16 ± 5 (10)	33 ± 15 (9)	36 ± 10 (9)	38 ± 6 (6)
$TP_{(R)}$	**H_1**	-	15 ± 14 (8)	27 ± 8 (7)	26 ± 10 (10)	41 ± 19 (9)	65 ± 14 (9)	70 ± 12 (6)
	H_2	-	16 ± 15 (8)	30 ± 8 (7)	29 ± 14 (10)	61 ± 18 (9)	59 ± 13 (9)	65 ± 21 (6)
$TP_{(Ef)}$	**H_1**	10 ± 5 (6)	5 ± 1 (8)	13 ± 3 (7)	11 ± 3 (10)	19 ± 6 (9)	11 ± 6 (9)	17 ± 12 (6)
	H_2	7± 8 (6)	5 ± 2 (8)	18 ± 4 (7)	12 ± 6 (9)	23 ± 6 (9)	19 ± 9 (9)	22 ± 4 (6)

Table S.8 – PO_4-P concentrations in influent digestate (in), HRAP (H), recirculation (R) and effluents (Ef) for the conventional HRAP ($HRAP_1$, H_1) and the LED-enhanced HRAP ($HRAP_2$, H_2) (Mean ± S.D (Data number))

Parameter		Stage						
		0	**I**	**II**	**III**	**IV**	**V**	**VI**
PO_4-$P_{(in)}$	**H_1**	15 ± 8 (4)	4 ± 3 (8)	17 ± 8 (7)	4 ± 1 (10)	17 ± 9 (9)	9 ± 5 (9)	9 ± 4 (6)
	H_2	16 ± 5 (4)	5 ± 3 (8)	14 ± 5 (7)	6 ± 3 (10)	16 ± 9 (9)	8 ± 3 (9)	8± 3 (6)
PO_4-$P_{H)}$	**H_1**	4 ± 0 (9)	3 ± 1 (8)	12 ± 3 (7)	8 ± 2 (10)	12 ± 7 (9)	8 ± 7 (9)	4 ± 4 (6)
	H_2	6 ± 1 (9)	4 ± 2 (8)	13 ± 4 (7)	9 ± 2 (10)	14 ± 10 (9)	6 ± 6 (9)	9 ± 4 (6)
PO_4-$P_{(R)}$	**H_1**	-	3 ± 3 (8)	9 ± 4 (7)	8 ± 5 (10)	13 ± 7 (9)	4 ± 5 (9)	6 ± 4(6)
	H_2	-	7 ± 6 (8)	14 ± 6 (7)	11 ± 6 (10)	19 ± 10 (9)	9 ± 9 (9)	7 ± 3 (6)
PO_4-$P_{(Ef}$	**H_1**	8 ± 4 (6)	3 ± 2 (8)	9 ± 4 (7)	7 ± 3 (10)	15 ± 5 (9)	7 ± 6 (9)	9 ± 5 (6)
	H_2	8 ± 4 (6)	3 ± 2 (8)	13 ± 3 (7)	10 ± 4 (10)	16 ± 6 (9)	14 ± 9 (9)	15 ± 3 (6)

Table S.9 – N and P content in the biomass, percentage of TN measured as TAN and N and P recovery factors measured in the waste biomass

Parameter		Stage						
		0	**I**	**II**	**III**	**IV**	**V**	**VI**
N recovery in WB (%)	H_1	0±0 (3)	9±4 (3)	8±3 (5)	17±6 (10)	13±7 (10)	15±10 (8)	13±9 (6)
	H_2	0±0 (3)	11±5(3)	11±11 (5)	14±12 (10)	6±4 (10)	23±8 (8)	34±11 (6)
P recovery in WB (%)	H_1	0±0 (3)	14±10 (3)	10±7 (5)	22±8 (10)	24±9 (10)	30±7 (8)	45±10 (6)
	H_2	0±0 (3)	13±3 (3)	5±4 (5)	29±19 (10)	14±6 (10)	34±13(8)	48±7 (6)
%TAN	In_1	54±62 (3)	67±16 (3)	71±11 (7)	77±25 (10)	71±11 (10)	70±16(6)	68±8 (5)
	In_2	65±21(3)	66±19 (3)	69±14 (7)	75±26 (10)	74±12 (11)	63±14(6)	78±15 (5)
	H_1	4±5 (3)	13±10 (3)	38±19 (7)	29±12 (10)	24±6 (11)	24±14(6)	31±13 (5)
	H_2	19±6 v	16±13 (3)	58±19 (7)	44±21 (10)	62±19 (11)	51±17 (6)	51±23 (5)

Table S.10 Free ammonia nitrogen (FAN) in the conventional HRAP ($HRAP_1$, H_1) and the LED-enhanced HRAP ($HRAP_2$, H_2) (Mean ± S.D (Data number))

Parameter		Stage						
		0	**I**	**II**	**III**	**IV**	**V**	**VI**
FAN (%)	**H_1**	80±14 (3)	57±38 (7)	3±2 (7)	5±5 (10)	1±1 (10)	1±1 (9)	1±0 (6)
	H_2	2±4 (3)	1±1 (7)	2±1 (7)	2±2 (10)	6±3 (10)	8±1 (9)	7±3 (6)
FAN (mg/L)	**H_1**	1.2±1.3 (3)	2.9±2.9 (7)	1.2±1.1 (7)	2.2±1.9 (10)	0.5±0.4 (10)	0.4±0.4 (9)	0.3±0.3 (6)
	H_2	0.1±0.1 (3)	0.1±0.1 (7)	1.8±1.2 (7)	0.8±0.5 (10)	11.9±6.7 (10)	15.5±6.6 (9)	12.8±8.4 (6)

Table S.11 Light attenuation (K_d) for Sunlight and LEDs, PAR (Daily surface irradiance) and E_{mix} values in the conventional HRAP ($HRAP_1$, H_1) and the LED-enhanced HRAP ($HRAP_2$, H_2) (Mean ± S.D (Data number))

Parameter		Stage						
		0	**I**	**II**	**III**	**IV**	**V**	**VI**
K_d *(sunlight)*	H_1	26 ± 4	44±6	78±12	87±43	96±25	112±9	109±6
	H_2	5±2	6±1	71±11	83±13	134±21	132±21	141 ± 27
K_d *(LED)*	H_2	10±1	16±2	45±4	68±2	93±16	114±13	-
Sunlight PAR (mol/d)	H_1	223±75	177±46	134±22	172±49	225±75	170±40	138±24
	H_2	54±3	43±2	33±1	42±0.1	55±0.3	42±0.1	34±0.1
LED PAR (mol/d)	H_2	1.151	1.151	1.151	2.014	2.014	2.877	-